

A TRIDENT SCHOLAR PROJECT REPORT

NO. 250

“Thermophotovoltaic Emitter Material Selection and Design”



UNITED STATES NAVAL ACADEMY
ANNAPOLIS, MARYLAND

This document has been approved for public
release and sale; its distribution is unlimited.

20031201 114

USNA-1531-2

REPORT DOCUMENTATION PAGE

Form Approved
OMB No. 074-0188

Public reporting burden for this collection of information is estimated to average 1 hour per response, including the time for reviewing instructions, searching existing data sources, gathering and maintaining the data needed, and completing and reviewing the collection of information. Send comments regarding this burden estimate or any other aspect of the collection of information, including suggestions for reducing this burden to Washington Headquarters Services, Directorate for Information Operations and Reports, 1215 Jefferson Davis Highway, Suite 1204, Arlington, VA 22202-4302, and to the Office of Management and Budget, Paperwork Reduction Project (0704-0188), Washington, DC 20503.

1. AGENCY USE ONLY (Leave blank)

2. REPORT DATE
7 May 1997

3. REPORT TYPE AND DATE COVERED

4. TITLE AND SUBTITLE

Thermophotovoltaic emitter material selection and design

5. FUNDING NUMBERS

6. AUTHOR(S)

Patrick C. Saxton

7. PERFORMING ORGANIZATION NAME(S) AND ADDRESS(ES)

U.S. Naval Academy
Annapolis, MD

8. PERFORMING ORGANIZATION REPORT NUMBER

USNA Trident Scholar project report
no. 250 (1997)

9. SPONSORING/MONITORING AGENCY NAME(S) AND ADDRESS(ES)

10. SPONSORING/MONITORING AGENCY REPORT NUMBER

11. SUPPLEMENTARY NOTES

Accepted by the U.S. Trident Scholar Committee

12a. DISTRIBUTION/AVAILABILITY STATEMENT

This document has been approved for public release; its distribution is UNLIMITED.

12b. DISTRIBUTION CODE

13. ABSTRACT: Direct energy conversion is an attractive option for the Navy because it eliminates the need for complex machinery and reduces maintenance concerns by eliminating moving parts. Thermophotovoltaic (TPV) generators offer all of the advantages of direct energy conversion, and can be run from waste heat. Current TPV generators are either inefficient or impractical. The focus of this research is to further technical understanding of the material issues involved in designing a TPV generator. Much like a solar power system, TPV generators use photocells to collect radiant energy and produce electric power. In this system, radiation is collected from a high temperature emitter material which emits photons with a wide spectrum of energies, the peak in the spectrum being directly related to the material temperature. Current TPV cell technology dictates that the emitter material needs to withstand 1300°C in a combustion gas atmosphere and achieve an emissivity of at least 0.90. Initial material screening included ceramics, refractories, metallics, and ceramic matrix composites. Candidate materials were selected based on available published data. Thermal shock and oxidation experiments were conducted, and materials were evaluated for emissivity in conjunction with NASA Lewis Research Center. Machinability, thermal conductivity, and thermal expansion properties were also considered. The most viable emitter candidates were determined to be C/SiC with SiC overcoat and SiC/Si.

14. SUBJECT TERMS

thermophotovoltaic, emitter, emissivity, high temperature materials, ceramic composites, refractory alloys

15. NUMBER OF PAGES

16. PRICE CODE

17. SECURITY CLASSIFICATION
OF REPORT

18. SECURITY CLASSIFICATION
OF THIS PAGE

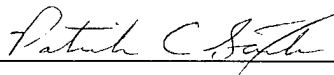
19. SECURITY CLASSIFICATION
OF ABSTRACT

20. LIMITATION OF ABSTRACT

“Thermophotovoltaic Emitter Material Selection and Design”

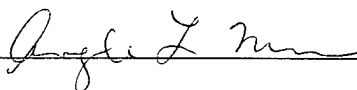
by

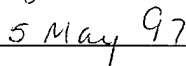
Midshipman Patrick C. Saxton, Class of 1997
United States Naval Academy
Annapolis, Maryland



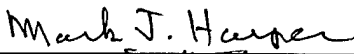
Certification of Advisors Approval

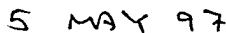
Assistant Professor Angela L. Moran
Mechanical Engineering Department





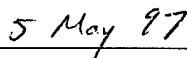
Associate Professor Mark J. Harper
Department of Naval Architecture, Ocean and Marine Engineering





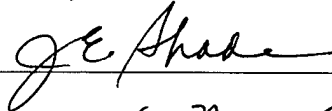
Associate Professor Keith W. Lindler
Department of Naval Architecture, Ocean and Marine Engineering





Acceptance for the Trident Scholar Committee

Professor Joyce E. Shade
Chair, Trident Scholar Committee





ABSTRACT

Direct energy conversion is an attractive option for the Navy because it eliminates the need for complex machinery and reduces maintenance concerns by eliminating moving parts. Thermophotovoltaic (TPV) generators offer all of the advantages of direct energy conversion, and can be run from waste heat. Current TPV generators are either inefficient or impractical. The focus of this research is to further technical understanding of the material issues involved in designing a TPV generator. Much like a solar power system, TPV generators use photocells to collect radiant energy and produce electric power. In this system, radiation is collected from a high temperature emitter material which emits photons with a wide spectrum of energies, the peak in the spectrum being directly related to the material temperature. Current TPV cell technology dictates that the emitter material needs to withstand 1300°C in a combustion gas atmosphere and achieve an emissivity of at least 0.90. Initial material screening included ceramics, refractories, metallics, and ceramic matrix composites. Candidate materials were selected based on available published data. Thermal shock and oxidation experiments were conducted, and materials were evaluated for emissivity in conjunction with NASA Lewis Research Center. Machinability, thermal conductivity, and thermal expansion properties were also considered. The most viable emitter candidates were determined to be C/SiC with a SiC overcoat and SiC/Si.

Keywords: thermophotovoltaic, emitter, emissivity, high temperature materials, ceramic composites, refractory alloys

ACKNOWLEDGEMENTS

I would like to express my gratitude to all those who helped me bring this project to its conclusion. Butch Antenucci, Steve Crutchley, Charlie Hoyt, thank you for always going out of your way to ensure that my testing equipment, travel orders, and computers were in order. Dr. Bruce Banks and Dr. Sharon Rutledge, thank you for your hospitality at NASA LeRC and for guiding me during the emissivity testing. Mr. Mike Kaspyrzak, thank you for always being willing to emergency ship additional material samples.

A special thank you to Dr. Larry Fehrenbacher and Dr. Mark Patterson for opening your doors to my shock testing and for offering invaluable advice and expertise. Professor Mark Harper and Professor Keith Lindler, thank you for your encouragement throughout the year, even as the deadlines loomed and passed. Tom, thank you for letting me borrow your computer equipment for weeks on end. Tim, your constant help throughout the project will not be forgotten. I must also thank my parents who never complained even though they have not seen me and have rarely heard from me in several months due to the demands of the project.

Finally, I want to offer my deepest gratitude to Professor Angela Moran. Your advice, guidance, and occasional prodding inspired me throughout the year and made this project what it was.

TABLE OF CONTENTS

Abstract	1
Acknowledgements	2
Table of Contents	3
Figures	5
Tables	7
1.0 Introduction	8
1.1 Objectives	8
1.2 Methodology	8
2.0 Thermophotovoltaic Background	10
2.1 The Fundamental Process	10
2.2 Previous Research	14
2.3 Applications	16
3.0 Initial System Design	17
3.1 Initial Design	17
3.2 Temperature Profile	19
3.3 Exhaust Gases	20
4.0 Materials Background	21
4.1 Metals	21
4.2 Refractory Metals	22
4.3 Ceramics	26
4.4 Composites	30
5.0 Emitter Material Properties	32
5.1 Melting Temperature	32
5.2 Emissivity	32
5.2.1 Fundamentals of Emissivity	33
5.2.2 Enhancing Emissivity	39
5.3 Corrosion Resistance	44
5.4 Thermal Expansion	45
5.5 Thermal Shock	45
5.6 Thermal Conductivity	46
5.7 Machinability	46
6.0 Preliminary Material Screening	47
6.1 Compiled Data	47
6.2 Material Information	48

7.0	Material Property Experimentation	56
7.1	Oxidation Experiment - Phase I	56
7.2	Thermal Shock Testing - Phase I	59
8.0	Material Selection	63
9.0	Property Verification and Quantification	66
9.1	Oxidation Testing - Phase II	66
9.2	Thermal Shock Testing - Phase II	69
9.3	Emissivity Testing	77
10.0	Final Material Selection	97
10.1	Material Properties	97
10.2	Weighting of Criteria	99
10.3	Emitter Material	102
10.4	Alternative Design	103
11.0	Conclusions	105
11.1	Design Evaluation	105
11.2	Material Recommendation	106
11.3	Project Conclusions	107
	Works Cited	108
	References	110

FIGURES

Figure 1	TPV Concept	12
Figure 2	Initial TPV System Design	18
Figure 3	Graphical Representation of Planck's Law	36
Figure 4	Boron Nitride Sample	49
Figure 5	C-103 Sample	50
Figure 6	Nb-1%Zr Sample	50
Figure 7	MA956 Sample	52
Figure 8	SiC Sample	53
Figure 9	SiC/Si Sample	54
Figure 10	Zirconia Sample	55
Figure 11	Alumina Sample	55
Figure 12	Initial Oxidation Test Samples	57
Figure 13	Initial Oxidation Test Results	57
Figure 14	Acetylene Torch and Pyrometer	69
Figure 15	Water Quenching	70
Figure 16	Shock Tested Boron Nitride	70
Figure 17	Shock Tested C-103	71
Figure 18	Shock Tested MA956	71
Figure 19	Shock Tested Nb-1%Zr	72
Figure 20	Shock Tested SiC	72
Figure 21	Shock Tested SiC/Si	73
Figure 22	Shock Tested WRe	73
Figure 23	Shock Tested Zirconia	74
Figure 24	Fractured Alumina Sample	74
Figure 25	Shock Tested C/SiC w/ SiC	74
Figure 26	Shock Tested ZrB ₂ /SiC	75
Figure 27	Shock Tested Woven C/SiC	75
Figure 28	Shock Tested CVD SiC/C	76
Figure 29	Shock Tested Silicon Nitride	76
Figure 30	Sample Holder	78
Figure 31	Emissivity Measuring System	78
Figure 32	Computer Display	78
Figure 33	Emissivity of Boron Nitride	80
Figure 34	Emissivity of Nb-1%Zr	81
Figure 35	Emissivity of Alumina	82
Figure 36	Emissivity of C-103	83
Figure 37	Emissivity of WRe	84
Figure 38	Emissivity of MA956	85
Figure 39	Emissivity of Silicon Nitride	86
Figure 40	Emissivity of Zirconia	87
Figure 41	Emissivity of SiC/Si	88

FIGURES (CONTINUED)

Figure 42	Emissivity of Oxidized SiC/Si	89
Figure 43	Emissivity of CVD SiC/C	90
Figure 44	Emissivity of CVD SiC	91
Figure 45	Emissivity of Woven C/SiC	92
Figure 46	Emissivity of CVD HfC	93
Figure 47	Emissivity of HfC-10%TaC	94
Figure 48	Emissivity of ZrB ₂ /SiC	95
Figure 49	Emissivity of C/SiC w/ SiC	96

TABLES

Table 1	Refractory Metal Coatings	25
Table 2	Candidate Material Properties	48
Table 3	Summary of Phase I Thermal Shock Test Results	62
Table 4	Composite Samples Obtained	65
Table 5	Summary of Phase II Oxidation Testing	68
Table 6	Phase II Thermal Shock Results	77
Table 7	Emissivity of Boron Nitride	80
Table 8	Emissivity of Niobium-1%Zirconium	81
Table 9	Emissivity of Alumina	82
Table 10	Emissivity of C-103	83
Table 11	Emissivity of WRe	84
Table 12	Emissivity of MA956	85
Table 13	Emissivity of Silicon Nitride	86
Table 14	Emissivity of Zirconia	87
Table 15	Emissivity of SiC/Si	88
Table 16	Emissivity of Oxidized SiC/Si	89
Table 17	Emissivity of CVD SiC/C	90
Table 18	Emissivity of CVD SiC	91
Table 19	Emissivity of Woven C/SiC	92
Table 20	Emissivity of CVD HfC	93
Table 21	Emissivity of HfC-10%TaC	94
Table 22	Emissivity of ZrB ₂ /SiC	95
Table 23	Emissivity of C/SiC w/ SiC	96
Table 24	Summary of Candidate Material Properties	98
Table 25	Material Property Weighting	99
Table 26	Weighted Quantitative Material Comparison	101

1.0 INTRODUCTION

The focus of this research was material selection for the emitter in a high temperature thermophotovoltaic (TPV) generator. This paper examines the TPV system and emitter requirements, background materials research conducted, experimental material results obtained, and the final material selection and emitter design.

1.1 OBJECTIVES

In order to meet acceptable efficiencies and lifetime expectancies, the thermophotovoltaic emitter meet specific criteria:

1. Operate at a temperature of 1300°C
2. Possess an emissivity greater than 0.90

Additionally the scope of the research mandated that the following be investigated:

1. Methods of measuring surface emissivity
2. Methods of enhancing surface emissivity
3. High temperature structural materials

1.2 METHODOLOGY

The objectives of this project were achieved through the following primary steps:

Background Research - A thorough review of previous TPV research and processes involved in TPV energy generation was conducted. Supporting research also included an involved study of materials and their associated properties.

Experimentation - Candidate materials were tested for oxidation resistance, thermal shock resistance, and emissivity in cases where the information was not available in the technical literature.

Material Selection - Final emitter material selection was based on TPV system requirements, data obtained through background research, and data obtained via experimentation.

2.0 THERMOPHOTOVOLTAIC BACKGROUND

Thermophotovoltaic energy conversion is attracting the engineering world's attention because it is a promising form of direct energy conversion. In the case of the TPV generator, this means that infrared thermal radiation is directly converted into electrical power with no moving parts. A close analogy can be drawn to photovoltaics, in which sunlight is directly converted to electrical energy. Direct energy conversion is advantageous because it is quiet, portable, and does not have the maintenance requirements of systems with moving mechanical components.

2.1 THE FUNDAMENTAL PROCESS

A TPV generator is composed of three main parts: a thermal radiator, a thermal radiation filter, and a semiconductor diode. In many instances the thermal radiation filter is incorporated into the semiconductor diode, called a TPV cell [1].

The fundamental idea behind a TPV generator is that a heat source is used to heat the emitter material up to an extremely high temperature. All materials emit radiation, but the magnitude of the emissions is determined by the temperature of the material, and is in fact a function of the temperature raised to the fourth power. The net radiation exchange between a material and its environment is then a function of the temperature of the material and the temperature of the environment. According to the Second Law of Thermodynamics, the net radiation exchange results in the high temperature emitter losing energy to its environment. The TPV cells are then positioned to collect this radiant energy.

The choice of material to serve as the emitter dictates the characteristics of the emitted radiation. Planck's Law reveals how an ideal material radiates energy as a function of its temperature, but no material is ideal [2]. Emissivity is the property used to quantify how closely a material models an ideal radiator, otherwise known as a blackbody radiator. It is the material's emissivity that determines how the emitter will radiate its energy at a given temperature. Accordingly, it is logical that an emitter is selected to match the TPV cells collecting this radiant energy. TPV cells can be tuned towards specific wavelengths of radiation, and hence system efficiency can be improved by matching a radiator to the collecting TPV cells.

It is extremely difficult to find an emitter whose emission spectrum matches the requirements of the TPV cells, so reflectors are utilized to reflect unuseable photons back to the emitter. There are two principal types of reflectors: selective filters and back-side reflectors.

The selective filter is placed between the emitter and collector cell, while the back-side reflector is attached to the back of the TPV cell. The selective filter is designed to allow photons with a wavelength that can be used by the TPV cell to pass through, while reflecting photons of other wavelengths back to the emitter. Reflected photons are reabsorbed by the emitter rather than being lost to the environment, improving the generator's overall efficiency. The use of tandem filters is one approach to selective filtering. In this approach a plasma filter is utilized to provide long wavelength reflectivity, while an interference filter is used to provide mid-infrared reflectivity. Short wavelengths are then allowed to pass through the filter. The interference filter provides

exceptional but limited reflectivity; therefore, the plasma filter is needed to compensate for the interference filter's limitations at longer wavelengths.

Back surface reflectors must be paired with TPV cells that are transparent to useless photons. Photons that cannot be utilized by the TPV cell pass through the cell, hit the reflector at the back of the cell, and return to the emitter. The difficulties with this method are that the reflector must adhere to the back of the TPV cell and must not have a high electrical contact resistance [1]. A typical TPV emitter, filter, and cell system is illustrated in Figure 1.

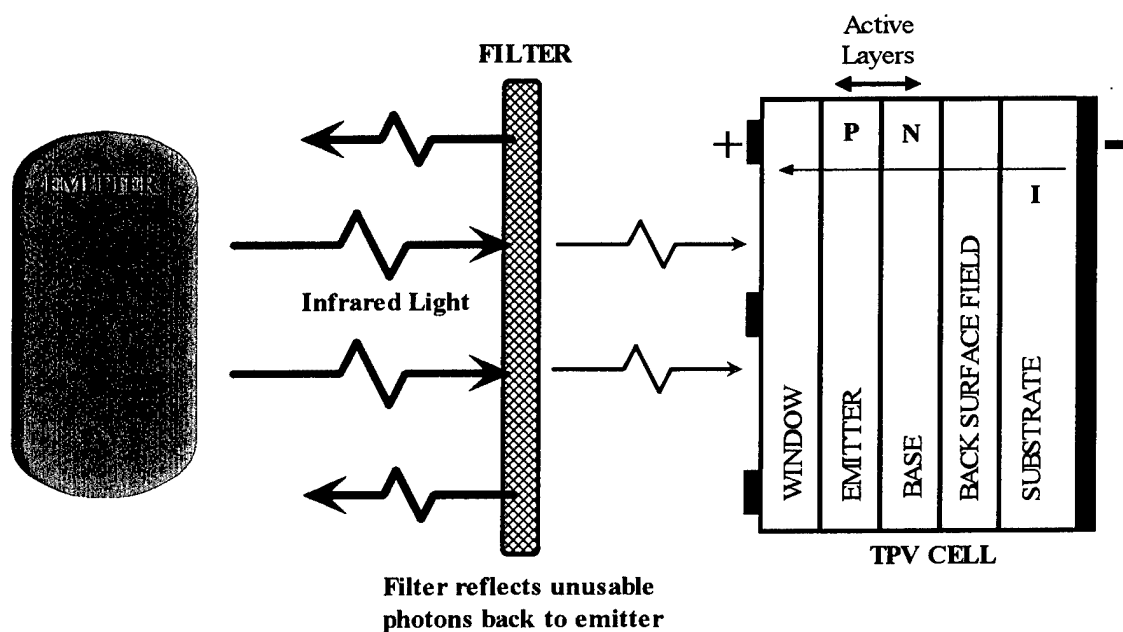


Figure 1 TPV Concept

The front contact is a series of metal layers deposited on the surface of the cell that maintain secure mechanical and electrical bonds to that surface. Often the front contact is composed of three layers: the adhesion layer, diffusion barrier layer, and

conductor layer. Usually the front contact covers approximately ten percent of the surface of the TPV cell, since covering any more of the surface will reduce the active area of the cell where photons enter.

The photons interact with the cell in the active layers, where they create charge carriers. If they reach the p-n junction, they are converted into usable power output. The active layers are composed of semiconductors, both n-type and p-type. N-type semiconductors conduct current with electrons in the conduction band, while p-type semiconductors conduct current with holes (an absence of an electron) in the valence band.

The window and back-surface field are added to the cell to help charge carriers reach the p-n junction, by preventing them from diffusing out of the base or emitter in the wrong direction. The substrate provides both a crystal seed from which to grow the single crystal active layers and a sound mechanical structure to prevent the cell from shattering. The back contact is used to complete the electric circuit through the TPV cell.

Most TPV cells use n-on-p architecture, meaning the n-type semiconductor is placed on top of the p-type semiconductor. The n-type layer is generally on the order of $0.025\text{ }\mu\text{m}$ in thickness in order to allow the photons to pass through and be absorbed in the p-type layer. The resulting electrons in the p-type layer then diffuse to the p-n junction, where they are accelerated by the resulting electric field through the n-type semiconductor to the front contact. TPV cells can be constructed in a p-on-n arrangement as well [1].

This represents only one design for a TPV cell. Currently, various organizations are working to perfect smaller, more efficient cells. Each new cell design may be tuned to a different photon wavelength from the previous one, thus altering the relationship between the emitter and the TPV cell. TPV generator design is proving to be an iterative process in which advances in one component of the generator necessitate changes in another component. In this project the TPV cells and filters were supplied to the Naval Academy, leaving the emitter material as the final variable. As is detailed later, the wavelength for which the cells are tuned determines the ideal emitter temperature. The rest of the design is focused on choosing that emitter material.

2.2 PREVIOUS RESEARCH

The concept of building a thermophotovoltaic generator is not a new one, but recently the effort has been escalating. Many different ideas and techniques have been attempted over the last ten years, and a majority of the work has been published at the annual National Renewable Energy Laboratory (NREL) Conference on TPV Generation of Electricity. Research has focused on various aspects of TPV generator technology, including emitter design, collector cell enhancement, and TPV applications. The following section presents a summary of research activities that pertain to this project.

JX Crystals Inc.'s design of a small air-cooled TPV electric generator, called the "Midnight Sun," was an important development. The small portable 100 W unit consisted of a silicon carbide emitter, GaSb collector cells in tandem with selective infrared filters, and cooling fins used to regulate the cell temperatures. The emitter was

heated to temperatures as high as 1400°C by combustion gases from a gas burner. This research demonstrated that working TPV generators can be constructed and verified the theory behind them. The significant difference between JX Crystals' and the Naval Academy's projects is that JX Crystals used a silicon carbide emitter which achieved at best an emissivity of 0.75, while USNA is attempting to find an emitter material that can achieve an emissivity of at least 0.90. The JX Crystals' published report on their silicon carbide emitter design provides valuable insight into emitter design [3].

Kent State University and NASA Lewis Research Center collaborated to produce a report on the effect of thickness and temperature on the performance of selective emitters. The paper focused on a rare earth YAG (Yttrium Aluminum Garnet) selective emitter. While the emitter achieved a maximum emissivity of only approximately 0.70, the report examined important emissivity concepts such as spectral emittance and radiative efficiency [4].

McDonnell Douglas Aerospace (MDA), NASA Lewis Research Center (LeRC), and Lockheed Martin Astro Space have all researched applications for TPV generator technology. Specific applications appear to be aimed at space power applications. MDA and NASA LeRC joined forces to investigate solar thermophotovoltaic systems, while Lockheed Martin is investigating radioisotope thermophotovoltaic (RTPV) generators. Both reports provide insight into TPV generator fundamentals [5,6]. The Naval Academy's TPV generator project is unique because it requires a high temperature design with an unusually high emissivity requirement.

2.3 APPLICATIONS

TPV applications are continually being devised because TPV energy conversion is a relatively new process to the engineering community. Applications which appear impossible today may be practical in the future. Because of this, it is difficult to speculate on every TPV application, but there are many applications that are presently attainable including:

- 1) Remote Electricity Supplies
- 2) Transportation
- 3) Co-generation
- 4) Electric-grid independent appliances
- 5) Enabling technology or novel system components
- 6) Space, aerospace, and military power sources [7]

3.0 INITIAL SYSTEM DESIGN

The initial TPV generator design requirements greatly influence material selection. The design of the system determines the properties that are required of the material components that constitute the system. In high temperature applications such as this, determining which portions of the design will experience varying temperatures is critical. The following is a brief overview of the United States Naval Academy's initial system design and the resulting material concerns.

3.1 INITIAL DESIGN

The TPV generator is ultimately intended for use with a T-58 gas turbine. The initial system is designed such that it uses a portion of the combustion gases from the gas turbine as a heat source. Figure 2 is a diagram of the initial TPV system design.

In this figure, it can be seen that the combustion gases are extracted from the combustion chamber of the T-58 by way of an extraction tube. This gas tube extends from the inside of the combustion chamber to the inside of the emitter. The pressure inside of the combustion chamber is approximately 827 kPa (120 psi), which is sufficient to force combustion gases through the narrow opening of the extraction tube. The combustion gases pass through the extraction tube and exit at the top. At this point the gases are re-directed back down along the outside of the extraction tube within the confines of the cylindrical emitter. The gases then exit through an exhaust port at the base of the emitter. The TPV cells are located in close proximity to the outside surface of the emitter in order to absorb the emitted radiation. Water cooled channels are placed

against the backside of the TPV cells to serve as heat sinks because the TPV cells are inefficient at temperatures in excess of 100°C .

The driving idea behind this design is the need for an even temperature distribution along the surface of the emitter. The TPV cells are tuned for a specific temperature, and hence efficiencies can be improved if the entire emitter is operating

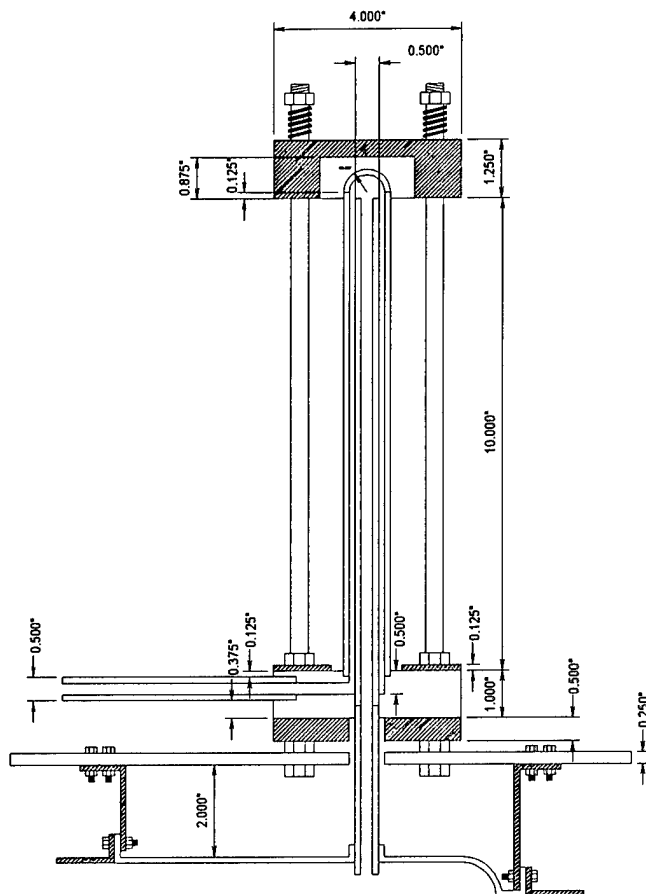


Figure 2 Initial TPV System Design

near this temperature. There are two primary modes of heat transfer from the gases to the emitter: radiation and convection. When the gas first enters the extraction tube it is at its hottest, and then it gradually cools as it progresses towards the top of the extraction tube. The temperature of the extraction tube will be directly related to this temperature profile, and so will the magnitude of the radiated heat from the tube to the inside of the emitter. Conversely, when the gases exit the extraction tube and progress down the outside of the tube towards the exhaust port, they will be hottest at the top and cooler as they descend. The heat transferred to the emitter by convection will be greatest at the top of the emitter and lowest at the bottom. The principle behind the design is that the heat transferred to

the emitter due to radiation and convection will balance each other, thus producing an even distribution.

From this design, critical components with specific material needs can be determined. The emitter must withstand high temperatures while also meeting other criteria such as a high emissivity, high temperature resistance, high oxidation resistance, and high thermal shock resistance. The extraction tube must be able to withstand the extreme temperatures of the combustion chamber, withstand the thermal shock that will result when the T-58 is ignited, and resist oxidation so that it does not fail inside of the combustion chamber. The end caps of the emitter prevent the combustion gases from escaping and coming into contact with the delicate TPV cells. These caps must be able to withstand high temperatures and not corrode. Additionally, the bottom end cap (or base plate) needs to be machinable to accommodate the intricate design.

3.2 TEMPERATURE PROFILE

An accurate temperature profile is critical in order to determine the specific temperature needs of the TPV generator components, particularly to determine the maximum temperature that the extraction tube experiences. Elevated temperatures can induce material phase changes as well as thermal stresses that can cause catastrophic failure.

The temperature profile for the combustion chamber was measured with tungsten-rhenium thermocouples. The T-58 gas turbine was run at various power levels while the thermocouples recorded the temperatures at several points in the combustion

chamber. As expected, maximum temperatures at all points occurred at the highest power level: 95%. Based on the initial design, materials placed in the combustion chamber see a maximum temperature of approximately 1090°C. Additional measurements indicated that combustion gases further downstream than the initial taps achieve much higher temperatures. The peak temperature of 1700°C occurred approximately one inch down stream of the initial tap [8]. An emitter material temperature of 1315°C is realistic if these 1700°C gases are tapped.

3.3 EXHAUST GASES

The composition of the combustion gases is also important. The composition of the gases affects the corrosion mechanisms that may result at high temperatures. At increasingly high temperatures, corrosion rates accelerate, which makes accurate identification of potential corrosion hazards vital. The chemical constituents of the T-58's combustion gas include:

- Carbon monoxide
- Carbon dioxide
- Water
- Hydrocarbons
- Nitrous oxide

4.0 MATERIALS BACKGROUND

Material selection is the primary limiting factor in thermophotovoltaic technology and performance. Each particular component of the TPV system has its own specific material requirements, which means that the best material for one application may not be the best for another application. The materials chosen will come from one of the four primary classes of candidate materials as defined for this project: metals, refractory metals, ceramics, and composites.

4.1 METALS

Metals are inorganic substances that are composed of one or more metallic elements and may also contain some nonmetallic elements. Iron, copper, and aluminum are three of the most common metallic elements. Frequently, non-metallic substances such as carbon, nitrogen, and oxygen appear in metallic substances as well. Typically, metals have a crystalline structure in which the atoms are arranged in an orderly manner. Metals are characterized as having high thermal and electrical conductivities, high strengths, and good ductility.

Metals are frequently alloyed with one another in order to produce substances with specific properties. Recent emphasis has been placed on alloying high temperature metals and creating "superalloys" [9]. These high temperature elements and alloys are considered to be a separate class of materials termed "refractory metals." The high temperature needs of this project eliminate the possibility of using common low temperature metals, but refractory metals offer a solution.

4.2 REFRACTORY METALS

Refractory metals refer to a group of metals having extremely high melting temperatures, such as molybdenum, niobium, tantalum, tungsten, chromium, vanadium, and rhenium. In a broad sense, this term refers to metals having melting points above that for iron, cobalt, and nickel. Originally these metals were used primarily for lamp filaments, electron-tube grids, heating elements and electrical contacts, but today many more applications have been developed. Aerospace, nuclear, electronics and chemical-process industries rely heavily on refractory metals. A majority of the total tonnage of refractory metals produced is now used in conjunction with aerospace applications [10].

Fabricability is the dominant factor in refractory metal selection. Niobium, tantalum, and their alloys are the most easily fabricated since they can be formed, machined, and joined by standard methods. They are easily machined primarily due to their high ductility, but also due to their high interstitial solubilities for carbon, nitrogen, oxygen, and hydrogen, which allow the material to absorb these embrittling contaminants. Niobium and tantalum lose their ductility at high temperatures, however, because they absorb too much of the embrittling contaminants. Because of this, protective coatings or atmospheres are necessary to protect niobium and tantalum from high temperatures. Molybdenum, tungsten, and their alloys require special techniques for fabrication. These materials have limited solubilities for carbon, nitrogen, oxygen, and hydrogen; therefore, the working environment must be carefully controlled to prevent embrittlement of the material [10].

Refractory metals have a high resistance to corrosion by liquid metals and aggressive acid solutions. Unfortunately, refractory metals are expensive. There are tradeoffs between corrosion resistance and cost effectiveness.

Refractory metals production begins with consolidation by melting or powder metallurgy techniques. Ingots and powder compacts are broken down by hot forging or extrusion into sheet, bar, and solid rounds for processing into sheet, plate, foil tubing, and bar products. Other techniques used for niobium and tantalum include vacuum electron beam melting.

Compared with traditional structural materials, refractories are generally difficult to machine. Equipment for machining these metals must be rigid and powerful in order to ensure optimum results. Frequently, carbide tools are required to ensure adequate tool life. All refractory metals can be joined by electron beam welding, gas tungsten-arc welding or resistance welding. Chemical changes due chiefly to atmospheric contamination and microstructural changes resulting from thermal cycling sometimes present problems. Electron beam welding has proven to be effective in achieving full weld penetration with an extremely narrow heat-affected zone, which minimizes the previously stated complications.

The following is a brief description of refractory metals that have significant applications:

Molybdenum Alloys — Initially molybdenum alloys were used exclusively by the space industry, but today they have far-reaching applications. They are now used in

thermal processing, electronic, nuclear, automotive, chemical, glass, specialty-alloy and metal-working industries. Molybdenum is recognized by its high melting point, high thermal conductivity, high resistance to corrosion, low specific heat, relatively low density, and low coefficient of thermal expansion. Due to a high ductile-to-brittle transition temperature, fabrication must be done at elevated temperatures. Molybdenum oxidizes rapidly at temperatures above 500°C; therefore, coatings are required for extended use above this temperature [10].

Niobium Alloys — Due to its relatively low density and excellent strength, niobium alloys have been used extensively in aerospace applications. Specifically, the alloys, C-103, C-129Y, and Cb-752 have been used as leading edges, nose caps, and rocket nozzles on re-entry vehicles. Niobium alloys are machined and welded with minimal difficulty, and maintain excellent strength at high temperatures. The alloys can be used in contact with liquid metals and some acids. One of the primary concerns is that coatings must be used at temperatures above 425°C [10].

Tantalum Alloys — Tantalum alloys have high melting points, good mechanical properties, and good fabricability. One drawback is tantalum's high density. Interstitial contents can be used to increase strength with an accompanied loss in ductility. Tantalum alloys can be extremely expensive. Tantalum oxidizes in air above 300°C, but it has excellent resistance to corrosion by acids and most liquid metals [10].

Tungsten Alloys - Tungsten has an extremely high melting temperature, but its high density, brittleness at room temperatures, poor fabricability, and poor oxidation resistance present many challenges to design engineers. Tungsten does have high tensile strength and good creep resistance, however. Frequently, tungsten is alloyed with thorium, molybdenum, and rhenium to produce a more ductile material [10].

Surface protection is the most significant obstacle to widespread use of refractory metals in high-temperature oxidizing environments. The present temperature limit of 1650°C is due primarily to the limitations of coatings. Coatings have insufficient life at reduced pressures and high temperatures in oxidizing environments and give unreliable protection, particularly at corners and edges of materials. Typical coatings used with refractory metals are summarized below in Table 1 [10].

Table 1 Refractory Metal Coatings

Coating Designation	Method of Application	Developer	Applicable Substrate	Temperature Limit (°C)
Aluminide Coatings				
LB-2 (Al-Cr-Si)	Fused slurry	GE	Niobium	1425
Al-Si-Cr	Fused slurry	Sylvania	Niobium	1425
Sn-Al	Slurry dip or spray	GT&E	Molybdenum	1480
Silicide Coatings				
Cr-Ti-Si	Vacuum pack	TRW	Niobium	1480
W Modified	Plasma spraying	TRW	Tungsten	1980

Table one is a small sampling of the coatings available to protect refractory metals from oxidation or other forms of corrosion. Coatings allow the refractory metals to operate at temperatures in excess of 1000°C.

4.3 CERAMICS

Ceramics by itself is a nebulous word. It is simple to give examples of ceramics, yet it remains difficult to define exactly what the word "ceramic" encompasses. There is a general conception (or misconception) that a ceramic is brittle, has a high melting temperature, is a poor conductor of heat and electricity, and is non-magnetic. For the purposes of this paper, ceramics will be defined as Loran S. O'Bannon defined them in Dictionary of Ceramic Science and Engineering: "Any of a class of inorganic, nonmetallic products which are subjected to a temperature of 540°C and above during manufacture or use, including metallic oxides, borides, carbides, or nitrides, and mixtures or compounds of such materials." Every ceramic expert seems to have his or her own slightly different definition, but this paper will clearly indicate the substances considered to be ceramics.

Within the broad class of ceramics there are many different classifications. Some classification schemes use material properties as the defining characteristic; others use applications as the defining characteristic; still others use chemical composition, mineral composition, and processing methods. For purposes of evaluating materials for use in specific areas of the TPV system, it is most convenient to classify materials based on their properties. For simple discussion it is easiest to classify materials by their chemical

composition. In any case, TPV research applies the materials typically classified as technical ceramics: ceramics that exhibit a high degree of industrial efficiency through their carefully designed microstructures and superb dimensional precision. Technical ceramics employ the use of selected materials with precisely regulated chemical composition, fabricated under strictly controlled methods of shaping and firing. "Advanced ceramics" is a further classification of technical ceramics, since advanced ceramics emphasize the advanced features that heighten the commercial value of technical ceramics. Advanced ceramics are then further broken down into structural ceramics, bioceramics, electroceramics, electronic ceramics, hydrothermal ceramics, and high performance ceramics. Generally speaking, TPV research focuses on structural ceramics, and additionally demands very specific material properties [11].

The following is a brief description of synthetic raw ceramic materials considered to have future significance. For organizational purposes, they are classified chemically.

Oxides:

Alumina (Al_2O_3) — Alumina is by far the most widely used synthetic raw material for ceramics. Additionally, alumina is extremely cost effective and abundant so it will most likely continue to be a popular raw material for ceramics production. Oxide ceramics typically have very strong ionic bonds. Of these materials, alumina has the most stable properties. Alumina can have vastly different physical properties depending on how it is produced. This is due primarily to the fact that alumina can have various

crystalline forms, impurities present in it, and particle diameters. Generally, alumina can be produced to match the material needs of an application [11].

Zirconia (ZrO_2) — Zirconia-based ceramics have seen many new developments of late. In its pure form, zirconia experiences a transition from a monoclinic system to a tetragonal system at 1100°C . The accompanying large change in volume can cause objects fabricated from zirconia to fail. This can be prevented by adding CaO , MgO or Y_2O_3 , which prevents this volumetric transition, thus forming stabilized zirconia. Zirconia is an extremely strong ceramic [11].

Magnesia (MgO) — Magnesia has a very high melting point: 2800°C . Unfortunately, it is also very reactive with water, carbon dioxide, and acids. In very specific applications with controlled environments, magnesia is used because of its high melting temperature [11].

Nonoxides:

Silicon Carbide (SiC) — Silicon carbide is an artificial material that contains strong covalent bonds. It demonstrates outstanding resistance to both high temperatures and corrosion. It is frequently used as an abrasive and refractory material. Japan produces more than 70,000 metric tons of SiC annually. SiC has attracted attention

recently as a new ceramic material because it is believed that SiC as an additive can manifest advanced features in other ceramics [11].

Silicon Nitride (Si_3N_4) — Silicon nitride is becoming more popular as an engineering ceramic. It is also a synthetic material with strong covalent bonding. Recently, higher grade materials and advanced production technology have enabled fine silicon nitride powders to be developed [11].

Boron Nitride (BN) — Boron nitride is another synthetic material, like silicon carbide and silicon nitride, although it cannot compare to their strength or abrasion-resistance. It has an unusually high thermal conductivity, a low coefficient of thermal expansion, and excellent thermal shock resistance. It is stable up to 3000°C in an inert atmosphere and is readily machinable. Boron nitride possesses outstanding resistance to corrosion up to 900°C [11].

Of these materials, alumina, zirconia, silicon carbide, and boron nitride are all candidates to be used as an emitter material and will be discussed later in this paper. Ceramics will also later be classified by their specific properties that satisfy the needs of the TPV system: high melting temperature, thermal shock resistance, low coefficient of thermal expansion, resistance to creep, high corrosion resistance, and high thermal conductivity.

4.4 COMPOSITES

Composite materials constitute a rapidly expanding class of materials. In general, a composite material is composed of a mixture or combination of two or more micro- or macroconstituents that differ in form and chemical composition and which are essentially insoluble in each other [9]. This means that two or more constituents can be combined to produce new materials that share the properties of the original constituents; a material can be created that takes advantage of specific properties of its components. Examples of common composites include concrete, asphalt, and wood.

Typically, a composite has some physically or chemically distinct phase contained within a continuous phase. The continuous phase is called the matrix, while the distributed phase is called the reinforcement phase. This reinforcement phase can be particles, whiskers, continuous fibers or sheets. Since composites can be composed of almost any material, they are difficult to classify. One common scheme focuses on the matrix phase, specifically the material that composes the matrix phase. Based on this scheme, there are three broad classifications: ceramic matrix composites, metal matrix composites, and polymer matrix composites.

At high temperatures, ceramic matrix composites (CMCs) are the most viable class of composites. CMCs take advantage of typical ceramic properties: high hardness, high strength, large modulus of elasticity, low density, low thermal expansion coefficients, and low thermal and electrical conductivity. The primary concern with ceramic materials is their low fracture toughness, which causes these materials to have little resistance to microcracks. The advantage of CMCs is that a reinforcement phase

can be used to increase the fracture toughness of the composite above that of the matrix material.

The most significant reinforcement phases used in CMCs are carbides, borides, nitrides, and oxides. The common characteristics of these four materials are high melting points, low density, high elastic modulus and high strength. Incorporation of these reinforcement materials in a ceramic matrix can introduce energy-dissipating phenomena such as debonding, crack deflection, and fiber pullout, which can significantly increase the toughness of the ceramic material.

Ceramic matrix composites have a multitude of applications, and the list continues to grow. The primary focus is on integrating CMCs into the aerospace and automotive industries. Currently, NASA is investigating the feasibility of an aerospace plane that would be able to fly from the earth's atmosphere into space and back again. Such a vehicle would require materials that could withstand temperatures in excess of 2000°C. The automotive industry could dramatically improve the efficiency of engines if they could maintain higher operating temperatures. Additionally, ceramic engines would be more compact, lighter, and would eliminate the need for complex cooling systems. Ceramic engineering is having an ever increasing affect on engineering and design, and ceramic matrix composites are at the forefront [12].

5.0 EMITTER MATERIAL PROPERTIES

The performance of the emitter is directly linked to the material from which it is constructed. The properties of that material thus influence the overall performance of the generator. Matching the emitter requirements to the properties of the material chosen is therefore critical. It is unlikely that one specific material meets every single requirement for the emitter. It is expected that the best material requires compromise. For example, one material may have a high melting temperature and emissivity but require a coating to provide for corrosion resistance. In any case, the important ideal emitter properties must first be identified and their significance weighted, before any compromises can be made.

5.1 MELTING TEMPERATURE

The material chosen must be able to withstand 1300°C without degrading. It is conceivable that the inside of the emitter may reach temperatures in excess of 1300°C during testing, so it is also important that there be some tolerance for even higher temperatures. Essentially, the higher the melting temperature the better. Some materials sublime rather than melt. This must also be avoided, since sublimation frequently reduces a material's emissivity.

5.2 EMISSIVITY

The objective of this research is to find a suitable emitter material that has an emissivity greater than 0.90. This value of 0.90 is dictated by current research in the field of direct energy conversion. High emitter emissivity is required to offset the

inefficiencies of TPV cells. Emissivity is not a property that is commonly known for most materials, particularly those most recently developed. It is important, therefore, to understand the fundamentals of emissivity in order to speculate as to which materials are worth investigating, since emissivity testing is both difficult and expensive.

5.2.1 Fundamentals Of Emissivity

Intuition indicates that a solid body existing in a vacuum that initially has a higher temperature than its surroundings will cool until it reaches thermal equilibrium with its environment. This cooling effect is due to the emission of thermal radiation from the surface of the solid body. While the solid body is emitting thermal radiation, it is also absorbing thermal radiation from its surroundings. The net heat transfer by radiation results in thermal equilibrium.

The emission from a body is a direct result of the energy released by the oscillations or transitions of the electrons in that body. The oscillations of the electrons are dependent on the internal energy of the body, which in turn is dependent on the temperature of the body. Radiation emerging from a finite volume of matter is the integrated effect of the local emission throughout the volume. In most solids, however, radiation emitted from interior molecules is rapidly absorbed by adjoining molecules. Therefore, radiation that actually escapes the surface of the body originates from the molecules that are within approximately $1\text{ }\mu\text{m}$ from the exposed surface. Due to this effect, radiative emission is viewed as a surface phenomenon for solids.

There are two theories on the transport mechanism of radiation: the propagation of a collection of particles termed photons and the propagation of electromagnetic waves. Standard wave properties and equations may be applied to radiation [2]:

$$\lambda = \frac{c}{\nu} \quad (1)$$

where:

$$\begin{aligned} \lambda &= \text{Wavelength (m)} \\ c &= \text{Speed of light (} 2.998 \times 10^8 \text{ m/s)} \\ \nu &= \text{Frequency} \end{aligned}$$

The common unit of wavelength is the micrometer, simply called a micron. The intermediate wavelengths of the electromagnetic spectrum, extending from approximately 0.1 to 100 microns, are generally called thermal radiation and are the primary focus of heat transfer.

Thermal radiation from a surface incorporates a range of wavelengths. The magnitude of the radiation has a spectral dependence, meaning that the magnitude varies with wavelength. Emitted radiation consists of a continuous distribution of monochromatic components. Ultimately, the magnitude of the radiation at a specific wavelength and the spectral distribution vary with the temperature of the emitting surface. Thermal radiation has a directional distribution in addition to its spectral

distribution, meaning that the magnitude of the radiation can vary with the direction of the emission.

Emissive power is a measure of the amount of radiation emitted from a surface per unit area. Emissive power can be calculated several different ways depending on whether the calculations take into account its spectral and directional dependence. In this project, the total hemispherical emissive power is calculated. Essentially, this means that the emissive power is calculated in all directions for all wavelengths. The total hemispherical emissive power is calculated by integrating the total spectral emissive power over the entire range of possible wavelengths [2]:

$$E = \int_0^{\infty} E_{\lambda}(\lambda) d\lambda \quad (2)$$

Generally, the term "emissive power" implies emissive power in all directions, thus the term "hemispherical" is considered redundant. For the purposes of this research, emissive power will refer to the total emissive power. One special case in which the directional distribution of emitted radiation can be automatically ignored is the diffuse emitter. By definition, the intensity of radiation emitted by a diffuse emitter is independent of direction.

A blackbody represents the ideal surface for a prescribed temperature and wavelength. No surface can emit more energy than a blackbody which is considered a diffuse emitter. Essentially, the blackbody is the perfect emitter to which the radiative properties of actual surfaces are compared. No surface can exactly match a blackbody, although close approximations can be achieved by cavities of uniform temperature. If radiation enters a small opening into a cavity, it is essentially reflected until it is

absorbed, and the only radiation that escapes through the opening is temperature dependent and emitted by the internal surfaces of the cavity.

The Planck Distribution defines the spectral distribution of blackbody emission. Since the blackbody is a diffuse emitter, the spectral emissive power can be determined by [2]:

$$E_{\lambda,b}(\lambda, T) = \frac{C_1}{\lambda^5 \left[\exp\left(\frac{C_2}{\lambda T}\right) - 1 \right]} \quad (3)$$

where:

C_1	=	Constant ($3.742 \cdot 10^8 \text{ W} \cdot \mu\text{m}^4/\text{m}^2$)
C_2	=	Constant ($1.439 \cdot 10^4 \mu\text{m} \cdot \text{K}$)
λ	=	Wavelength (μm)
T	=	Temperature (K)

This equation determines the Planck Distribution, as seen in Figure 3:

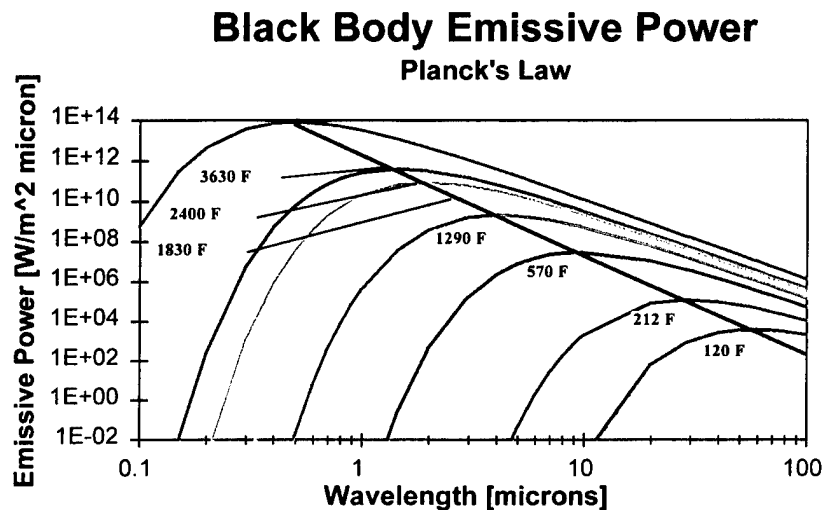


Figure 3 Graphical Representation of Planck's Law

From the distribution several important facts may be determined.

1. The emitted radiation varies continuously with wavelength.
2. At any wavelength the magnitude of the emitted radiation increases with increasing temperature.
3. The spectral region in which the radiation is concentrated depends on temperature, and hence the peak emitted wavelength depends on temperature.

The relation that determines the temperature dependence of the peak emitted wavelength is contained in Wein's displacement law [2]:

$$\lambda_{\max} T = C_3 \quad (4)$$

where:

$$\begin{aligned} \lambda_{\max} &= \text{Peak wavelength } (\mu\text{m}) \\ T &= \text{Temperature (K)} \\ C_3 &= \text{Constant } (2897.8 \mu\text{m}\cdot\text{K}) \end{aligned}$$

According to Wein's displacement law, the maximum spectral emissive power is displaced to shorter wavelengths with increasing temperature. For this research, the peak emitted wavelength of an ideal emitter can be determined for the operating temperature of 1300°C. Calculations reveal that the peak emissions occur at 1.86 microns, placing them in the infrared portion of the electromagnetic spectrum.

Since a blackbody is an ideal emitter for a given temperature, it is used as a reference in determining the emission from a real surface. Emissivity is defined as the ratio of the radiation emitted by the surface of a real material to the radiation emitted by a blackbody at the same temperature according to Wein's displacement law. Therefore, emissivity always has a value between 0 and 1. Obviously, the emissivity of a material can vary depending on whether the emission is being measured at one wavelength or in one direction or in wavelengths integrated over wavelength and direction, since a real surface is not necessarily a diffuse emitter. As with emissive power, the emissivity of a surface for the purposes of this research is determined by calculating the total hemispherical emissivity of the surface [2]:

$$\varepsilon(T) \equiv \frac{E(T)}{E_b(T)} \quad (5)$$

where:

$\varepsilon(T)$	=	Emissivity as a function of temperature (K)
$E(T)$	=	Total emissive power (W/m^2)
$E_b(T)$	=	Total emissive power of a blackbody (W/m^2)

The requirement for the emitter material is that it have an emissivity of 0.90. There are distinct advantages and disadvantages for determining the spectral emissivity of sample materials as opposed to total emissivity. Spectral emissivity measurements for each sample gives an excellent indication of the material's emissive properties at the

specific wavelength that the TPV cells are tuned: 1.86 microns. At the same time, should the TPV cells ever be improved to the point that an emitter could be operated at a lower temperature thus generating a different peak emitted wavelength, new data would have to be acquired at this new temperature and a new emitter material may be needed. If total emissivity is determined, a broader picture of the material's overall emissivity would be available. It is highly unlikely that the material would have an emissivity near 0.90 at the specified wavelength, 1.86 microns, since the material would have to be near blackbody across the entire spectrum (specifically at the peak wavelength emitted) in order to even approach a total emissivity of 0.90. Unfortunately, a sample that meets the required emissivity of 0.90 at the peak emitted wavelength may fall short for total emissivity, and thus be discarded when it should be considered a candidate material. Ideally, candidate samples are tested for both spectral emissivity and total emissivity. The equipment used to measure emissivity for this work is located at NASA Lewis Research Center.

5.2.2 Enhancing Emissivity

Often when high emissivities are required, materials must have their emissivities enhanced. Since the emissivity of a material is a function of the character of its surface, techniques for enhancing a material's emissivity focus on altering its surface. There are two main approaches to altering the surface of an emitting material: texturing the surface and coating the surface.

NASA Lewis Research Center in Cleveland, Ohio, has developed three techniques for enhancing surface emissivity via texturing. The three principle techniques are sputter etching, sputter texturing, and arc texturing [13,14].

Sputter etching is the process of removing material from a surface by bombarding it with a stream of high energy ions or neutral particles. Surface atoms and molecules are ejected from the surface of the target material due to interactions with the bombarding particles. Essentially, the end result is a surface that is highly pitted. In conjunction with this technique, a process termed "masking" may be used. A sputter mask is basically a mesh constructed of a material that is more sputter resistant than the target material. The mask protects areas of the target from sputtering and allows the surface of the target to be selectively textured according to the pattern of the mesh masking. Further research has allowed NASA to define the sputter etch rates of specific materials [14].

Sputter texturing is in many ways similar to sputter etching. The primary difference lies in the target material. The fundamental idea behind sputter texturing is that the surface material has distinct spatial variations in its sputter yield, meaning that different regions of the target material ejects more atoms when exposed to the ion beam. Ultimately, this creates the texture since areas of the surface over time have ejected significantly more atoms than neighboring regions. This technique is particularly effective for metal alloy targets. Metal alloys are by nature heterogeneously mixed, which means that regions of the surface are composed primarily of one type of metal atom while other regions are primarily composed of a different type of metal atom, thus

creating the potential for different sputter yields depending on the region of the surface that is being examined [14].

In cases where the target surface is a homogenous pure material, sputter texturing can still be used as long as the surface is seed textured first. Seed texturing is similar to sputter deposition, where atoms or molecules of one material are deposited on the surface of another. If the seeded atoms or molecules are then allowed to nucleate into segregated microscopic sites of sputter resistance on the target surface, sputter texturing can then be performed on the newly seeded surface.

In some specific cases, sputter texturing can be performed directly on homogenous pure materials, assuming that small voids exist in the bulk of the target material. These voids can then be exposed by the ion beam used in sputter texturing.

Arc texturing is a process used with metals in which carbon arc electrical discharges are struck across the surface of a metal inducing a change in morphology. Essentially, metal from the surface and carbon from the electrode vaporize during arcing and then condense again on the surface of the metal to create a rough surface with enhanced emissivity. Arc texturing is an excellent method for enhancing the emissivity of a metal [13].

The concept behind applying a coating to a material's surface to enhance its emissivity is obvious. If a material has a low emissivity, its emissivity may be enhanced by applying a thin layer of another material that has a higher emissivity. The difficulty in this technique lies in matching the proper coating with a material. Just as in alloying metals and joining materials, some materials respond favorably to coatings while others

do not. Sputter deposition is a technique used by NASA Lewis Research Labs to coat materials. It is a process by which material that is sputter etched from a target is accumulated on the surface of another material. Sputter deposition was previously developed using other techniques, but NASA is the first to develop ion beam sputter deposition. Essentially sputter deposition is similar to sputter etching except that the goal is to use the ejected atoms and molecules from the sputter etching process rather than to actually etch the material [14].

Thus far it has been implied that textured surfaces naturally have higher emissivities than non-textured surfaces. This is only true as long as the average width of the pits on the surface of the emitting material is several times larger than the wavelength of the emitted radiation of interest, which for this research is 1.86 microns. If this is true, then the small cavities in the surface of the textured material act as blackbody cavities. Incident radiation enters these cavities, is subsequently reflected inside the cavity and absorbed, then re-emitted as radiation with the peak emitted wavelength corresponding to the temperature of the emitter surface. This texturing causes the emitter surface to closely resemble that of a blackbody which enhances the overall emissivity of the material [14].

In some cases, it is possible to combine sputter processes with coating technology to further enhance the emissivity of a material surface. This is not always just as simple as adding a coating to a textured surface. It is important that the coating be exactly matched to the surface to be textured. It is also important to consider the environment to which the material's surface is exposed. At low temperatures it is much simpler to get

coated and textured surfaces to perform, but at high temperatures, materials naturally corrode at much higher rates. At extremely high temperatures, many materials naturally corrode in free air environments. Most of the materials that are easily sputter coated also naturally corrode at high temperatures (i.e. graphite and carbon-carbon composites). Even if the material does not directly corrode in the high temperature environment, creep (i.e. plastic deformation at elevated temperatures) can reduce the materials emissivity over time. Sometimes the texturing may begin to creep under its own weight, thus causing the peaks in the texturing to gradually settle into the cavities that initially enhanced the surface's emissivity. The net result is that the cavities begin to disappear, the surface degrades, and the net emissivity of the material is restored to near its initial untextured value.

Coatings can sometimes be applied to the surfaces of these materials to prevent corrosion and creep, and in specific cases the coatings may also enhance the emissivity of the material. However, when the material has been textured, it is nearly impossible to completely coat the surface of the material as there are pinholes in the coating, since the coating material can not fully penetrate the small cavities caused by the texturing process. When exposed to a high temperature environment, these pinholes rapidly develop into corrosion sites. Since this research involves operating the emitter material in extremely high temperature environments (1300°C), it may not be practical to attempt to combine coating technology with sputter technology. Ideally, the emitter material needs to be a material that does not require texturing to enhance its emissivity and can withstand the environment without a coating. If this is not possible, it is preferable that an emitter

material be used that withstands the environment after texturing. Texturing may not be necessary as long as a coating material can be identified that both enhances the material's emissivity and protects it from corrosion. In any case, it is best to avoid trying to match a coating to a textured surface in an attempt to protect the surface from corrosion.

5.3 CORROSION RESISTANCE

At 1300°C, most materials degrade quickly and easily. As mentioned in the previous section, material coatings can be used to enhance emissivity and provide corrosion protection. An emitter coating has to simultaneously enhance emissivity and corrosion resistance, due to the difficulty of coating a material that has had its surface emissivity previously enhanced through texturing.

Another alternative is to shield the emitter material from corrosive environments. This could be accomplished by fitting the inside of the emitter with a corrosion resistant cylindrical tube, and encapsulating the outside in a vacuum. There are far more materials that can withstand 1300°C in a vacuum than can withstand it in a free air environment.

If absolute corrosion resistance cannot be provided, then it may be necessary to compare each potential material's corrosion rate. In this scenario, the goal is to choose the emitter material that lasts the longest. This enables the overall design to be tested until an improved emitter is discovered.

5.4 THERMAL EXPANSION

The ideal emitter requires a low coefficient of thermal expansion. Thermal expansion does not directly affect the performance of the emitter, but it influences the design of the overall TPV generator. At 1300°C, thermal expansion can be considerable. If steps are not taken to allow for this expansion, considerable stresses develop in the emitter material, possibly causing catastrophic failure of the emitter. In the current design, springs are located at the top of the generator to account for the thermal expansion of the emitter. Ideally, if thermal expansion can not be minimized, thermal expansion coefficients of neighboring materials should match. This allows for the entire structure to expand in unison. This is particularly critical in regions where materials are tightly fitted together, such as the end caps that are used to seal the emitter tube.

5.5 THERMAL SHOCK

When the T-58 gas turbine is ignited, combustion gases immediately impinge on the drawing tube and emitter assembly of the generator. This sudden surge from a room temperature free air environment to a 1600⁺°C gaseous environment can cause catastrophic failure via thermal shock in many materials. This failure is due to the material experiencing rapid thermal expansion, which induces extreme stress. Some materials' crystal structures alter at high temperatures, causing a significant volume change resulting in structural failure. Typically, materials with low coefficients of thermal expansion are more resistant to thermal shock.

5.6 THERMAL CONDUCTIVITY

The thermal conductivity of the emitter directly affects the efficiency of the TPV generator. It is very difficult to heat the emitter up to 1300°C with the combustion gases of the T-58 generator due to the low convection coefficient of most gases. If the emitter is a poor thermal conductor, the outside of the emitter may not reach 1300°C due to the large temperature gradient. The emissive power of the emitter is a direct function of the outside surface temperature. The overall generator's efficiency can be drastically reduced if a large temperature difference exists between the inside and outside walls.

Conversely, it is important that other components in the TPV system have low coefficients of thermal conductivity. For example, heat conducted through the end-caps of the emitter should be minimized, since it is in essence energy wasted.

5.7 MACHINABILITY

Many of the emitter candidate materials are difficult to machine. This inherently limits the geometry of the emitter. Since most materials can be manufactured cylindrically, a cylindrical emitter seems most practical.

The machinability of the materials chosen for the other generator components is also a consideration. For example, the bottom end-cap to the emitter requires openings for the extraction tube and exhaust tube, and a groove to provide a seal for the bottom of the cylindrical emitter; therefore, the material selected needs to be highly machinable.

6.0 PRELIMINARY MATERIAL SCREENING

Preliminary evaluation of a wide variety and large number of materials was performed. The goal was to select several potential materials from each class of materials and gather published data concerning critical properties. From this listing, candidate materials were chosen for further testing.

6.1 COMPILED DATA

Table 2 lists the high temperature materials that were considered after an initial screening. The materials were chosen from several classes in order to ensure that a wide range of materials were evaluated experimentally. The classes represented include monolithic ceramics, refractory alloys, and composite materials. Traditional metals were eliminated since they would not be able to satisfy the high temperature requirements. The data in the table were obtained primarily from reference books, but a limited amount of data was taken from product literature.

Table 2 Candidate Material Properties

Candidate Material	Thermal Conductivity	Emissivity (Max)	Thermal Expansion	Oxidation Resistance	Melting Temp	Thermal Shock Resistance
	W/m-K	0.0 - 1.0	$\mu\text{m/mK}$	Poor \rightarrow Excellent	$^{\circ}\text{C}$	Poor \rightarrow Excellent
BN	< 0.6 @ 500 $^{\circ}\text{C}$		0.6	Poor above 900 $^{\circ}\text{C}$	3000	
C103	41.9		8.10		> 1315	
C/C Composites	0.05 – 0.40	~ 0.96	1 – 10		> 1315	
MA 956	27 @ 1100 $^{\circ}\text{C}$		15.5	Fair (produces oxide coating)	1482	
SiC (β)	71	~ 0.80	4.5		2200	
SiC / Si	~ 71		4.2		> 1315	
WRe	~ 100		~ 5		> 1315	
ZrO ₂	~ 10		10.5	Excellent	2715	
Nb-1%Zr	41.9	~ 0.95	7.54		2400	
Al ₂ O ₃ - α	29.0		5	Excellent	2050	

As indicated, limited data is available in the literature, requiring subsequent experimental property evaluation.

6.2 MATERIAL INFORMATION

A detailed description of each candidate material is listed below:

Boron Nitride (BN)

Boron nitride is similar to graphite in its structure and material properties. It possesses very high thermal conductivity and a very low thermal expansion coefficient, which leads to excellent thermal shock resistance. Boron nitride is stable up to 3000°C in an inert atmosphere and up to 900°C in air. Up to 900°C, it has high resistance to corrosion. Another advantage of boron nitride is its excellent machinability. Unlike graphite, boron nitride is an electrical insulator and is frequently used as a lubricant, high temperature structural material, and neutron absorption material [9].

The boron nitride used in this research was purchased from Advanced Ceramics Corporation. The sample was a hot pressed, pyrolytic, boron nitride powder cylinder measuring 12 inches in length and 1 inch in diameter. The sample (Figure 4) was opaque white with a chalky texture.

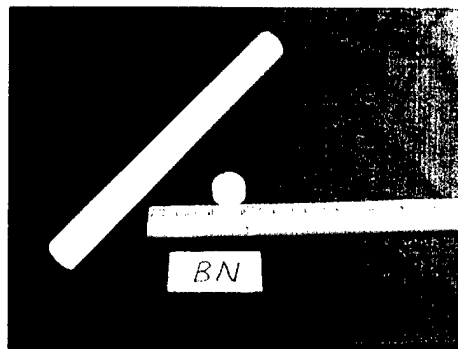


Figure 4 Boron Nitride Sample

C-103 (89Nb-10Hf-1Ti)

C-103 is a niobium based metal alloy used in high temperature applications. Specific applications include thrust chambers and radiation skirts for rockets and engines, guidance structure for glide re-entry vehicles, and thermal shields. In extreme temperatures, coatings are required to prevent degradation [10].

The C-103 sample used in this research was purchased from Teledyne. The sample was a hollow cylinder measuring 12 inches in length, with a 1.125 inch outside diameter and 1 inch inside diameter. It was a dull silver and smooth to the touch as shown in Figure 5.

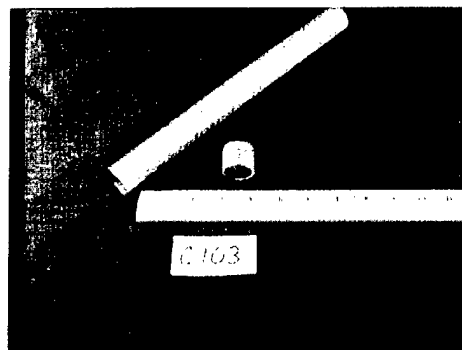


Figure 5 C-103 Sample

Nb-1%Zr

Nb-1%Zr is a niobium based metal alloy used in high temperature applications such as thermal barriers, liquid metal containers, nuclear applications, and sodium or magnesium vapor lamp parts. The melting temperature is approximately 2400°C. The coefficient of thermal expansion is approximately 7.54 $\mu\text{m/mK}$, and the thermal conductivity is approximately 41.9 W/mK at 25°C. Values at 1300°C can be extrapolated from the known information. Nb-1%Zr has shown signs of abruptly losing strength and ductility when exposed to 980°C for up to 500 hrs [10].

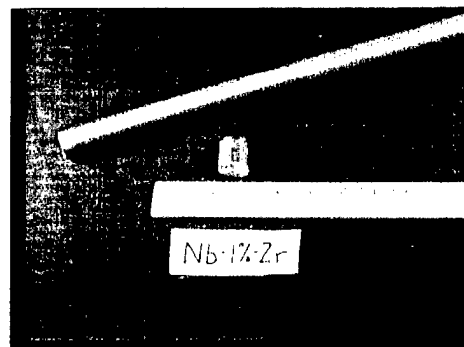


Figure 6 Nb-1%Zr Sample

The Nb-1%Zr sample used in this research was purchased from Cabot Corporation.

It was a solid rod measuring 51.25 inches in length with a 1 inch diameter. The sample was dull silver as shown in Figure 6.

MA956

INCOLOY alloy MA956 is an oxide-dispersion-strengthened, iron-chromium-aluminum alloy produced by mechanical alloying. The alloy is strengthened by an yttrium oxide dispersoid that remains stable at temperatures up to the melting point of the material. The nominal chemical composition of MA956 by weight is:

Iron	74%
Chromium	20%
Aluminum	4.5%
Titanium	0.5%
Yttrium Oxide	0.5%

The melting temperature is approximately 1482°C. The coefficient of thermal expansion is 15.5 $\mu\text{m}/\text{m}^\circ\text{C}$ at 1100°C. By linear extrapolation this value is expected to be near 16.5 $\mu\text{m}/\text{m}^\circ\text{C}$ at 1300°C. The thermal conductivity is approximately 27.0 W/m°C at 1100 °C. The longitudinal yield strength is approximately 76 MPa at 1200°C. This value is expected to decrease further as temperatures approach 1300°C. The transverse yield strength is approximately 72 MPa at 1200°C, but is also expected to decrease as the temperature increases. The high-temperature corrosion resistance of MA956 results primarily from the formation of a stable, tightly adherent oxide coating. Pre-oxidation treatment allows the material to be used in highly corrosive environments. Specific applications of INCOLOY alloy MA956 include gas-turbine combustion chambers, components of advanced energy systems, and other applications involving rigorous service conditions [15].

The material samples used in this research were obtained from Inco Alloys International. The samples were cylindrical rods, 12 inches long with 1 inch diameters. The rod seen in Figure 7 had a dull dark gray appearance on the outside but a shiny metallic silver appearance on the ends where they had been machine cut.

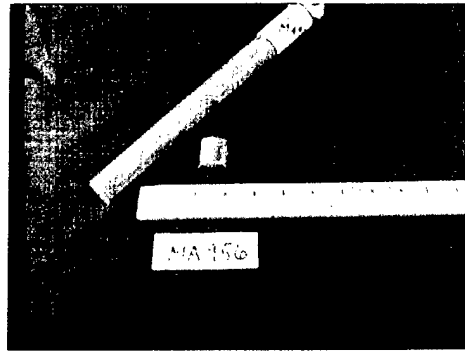


Figure 7 MA956 Sample

Silicon Carbide (SiC)

Silicon carbide ceramics have the important properties of high hardness, chemical inertness, abrasive resistance, and outstanding oxidation resistance at high temperatures. SiC is relatively brittle with low fracture toughness and can be difficult to produce. Typically, SiC is manufactured by infiltrating a powder compact of SiC and carbon with molten silicon, which reacts with the carbon to form more SiC, thus bonding the original SiC grains together. Most applications for SiC ceramics utilize their high hardness, chemical resistance, and abrasion resistance. These applications include use as seals and valves in the chemical industries, lens molds, rocket nozzles, wear plates for spray drying, and wire dies. They are also used as thrust bearings, ball bearings, pump impellers, and extrusion dies. Typically, SiC is used for rocket nozzle throats, heat exchanger tubes, and diffusion furnace components due to its heat and creep resistant characteristics [16].

The silicon carbide samples used in this research were purchased from Vesuvius. The samples were dense silica bonded silicon carbide flanged tubes. The typical chemical composition of these samples is:

Silicon Carbide	86.10%
Silica	11.75%
Alumina	0.78%
Iron Oxide	1.05%
Lime	0.21%
Magnesia	0.10%
Alkalies	Trace [17]

The tubes measured 12 inches in length, with a 1.75 inch outer diameter and 1 inch inner diameter. The samples were a brownish gray with random gray splotches on the outside as seen in Figure 8.

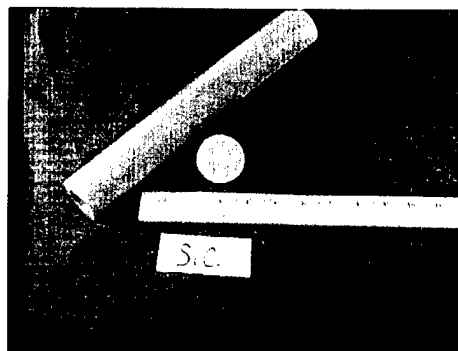


Figure 8 SiC Sample

Silicon Carbide in a Silicon Matrix (SiC/Si)

Silicon carbide in a silicon matrix is a ceramic composite used specifically for high temperature applications. The material has a melting point greater than 1600°C and demonstrates a reliable long life at temperatures as high as 1300°C. SiC/Si can withstand most corrosive environments, while providing good fracture toughness and resistance to

thermal shock, oxidation, and creep without extreme brittleness. The strength of this material increases with temperature, reaching 72 MPa at 1350°C. The coefficient of thermal expansion is 7.6 $\mu\text{m/mK}$. Applications have included annealing, carburizing, carbide solution treating, neutral hardening, carbo-nitriding, and ferriticnitrocarburizing in a wide range of atmospheres including endothermic, enriched gasses, ammonia enriched gasses, nitrogen, and mixed endothermic / ammonia. [18]

The SiC/Si used in this research was donated by INEX Incorporated. Several segments of various tubing were evaluated. Samples tested included 2.375 inch and 2.750 inch outer diameter segments, with 0.125 inch wall thicknesses. The samples were a medium gray color and the outside surfaces were textured as seen in Figure 9.

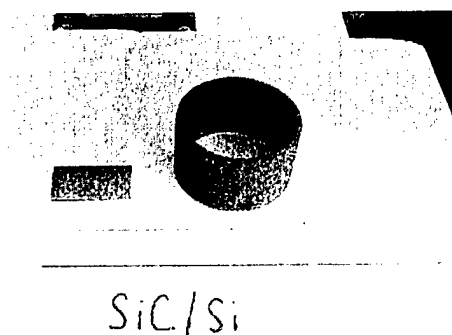


Figure 9 SiC/Si Sample

Zirconium Oxide / Yttrium Oxide (90% ZrO_2 - 10% Y_2O_3)

Pure zirconium oxide is polymorphic and transforms from a tetragonal to monoclinic structure at about 1170°C. The accompanying volume expansion makes it subject to cracking. The cubic structure can be stabilized at room temperatures, however, if refractory oxides are introduced, specifically Y_2O_3 . The stabilized form of zirconium oxide has a thermal conductivity of approximately 2.1 W/m-K at 1300°C [9].

The zirconia used in this research was ordered from Vesuvius McDanel. The 10.5 wt% yttria stabilized zirconia was ordered in 1 inch tubes, with an outer diameter of 1 inch and an inner diameter of 0.75 inches. The samples were glossy white, and smooth to the touch as seen in Figure 10.

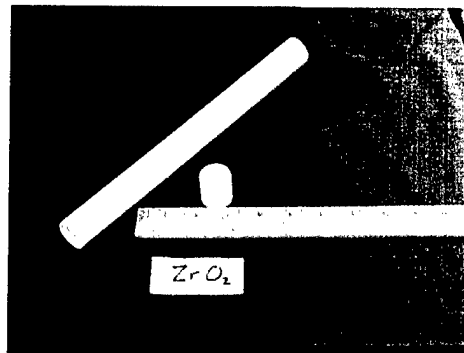


Figure 10 Zirconia Sample

Aluminum Oxide

Aluminum Oxide, commonly referred to as alumina, can be used in high temperature oxidizing and reducing environments. It is stable in these environments up to 1950°C. Like many ceramics, alumina is extremely brittle [9].

Samples for this research were obtained from Zircar. Samples include an 18 inch by 24 inch by 0.25 inch sheet as seen in Figure 11, and a 4 inch outer diameter, 3 inch inner diameter, 12.5 inch long cylinder.

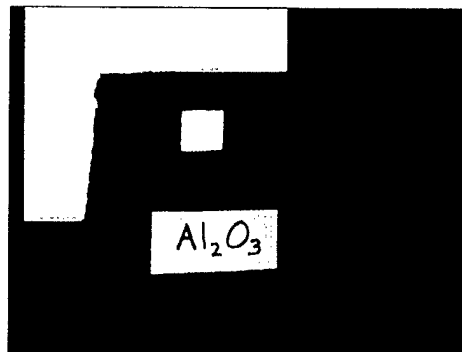


Figure 11 Alumina Sample

7.0 MATERIAL PROPERTY EXPERIMENTATION

Once the candidate emitter materials were selected, initial testing was conducted in order to determine which materials best met the criteria. Additional testing was conducted on these materials alone to limit costs and time.

Initial tests were either pass or fail. In the process of testing for potential emitter materials, consideration was given to whether a material may also function as a structural material. Materials that were completely eliminated from subsequent testing were those materials that can not be used for either the emitter or the structural components of the TPV assembly.

7.1 OXIDATION EXPERIMENT — PHASE I

The objective of the experiment was to evaluate how ten samples of different materials responded to exposure to a 1300⁺°C free air environment. Samples of the following materials were placed in the Thermolyne furnace at 1315°C:

C103	MA958	Nb-1%Zr
W-Re	BN	Al ₂ O ₃
ZrO ₂	SiC	Si/SiC
BN w/ Pd and Ag coating		

The ten samples were first weighed individually on a digital scale that was read to the thousandths of a gram. Meanwhile, the furnace was preheated to 1315°C. After the samples were weighed, they were placed on a piece of firebrick that measured approximately 2 inches by 4 inches by 5 inches. The materials were placed on one of the

4 inch by 5 inch faces such that they were near each other but not actually touching as seen in Figure 12. Once the furnace was up to temperature, metal tongs were used to place it in the furnace.

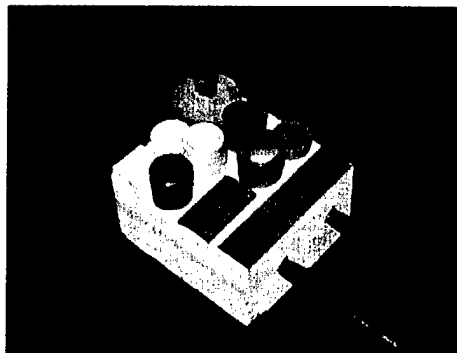


Figure 12 Initial Oxidation Test Samples

After one hour, the furnace door was opened and preparations were made to remove the samples. After inspecting the firebrick and samples, it was apparent that at least two of the materials had burned their way through the firebrick and had fallen off onto the ceramic tray in the bottom of the furnace. The metal tongs

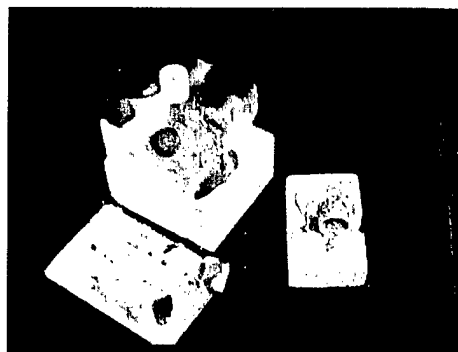


Figure 13 Initial Oxidation Test Results

were used first to remove the firebrick and samples that remained on it. Next, one of the samples that had fallen was easily grasped by the tongs, removed from the furnace, and placed on a spare piece of firebrick. The second sample that had fallen was stuck to a portion of the ceramic tray in the bottom of the furnace, so the entire portion of the tray was removed, including the sample that was stuck to it. The samples were then allowed to cool to room temperature.

Further inspection of the firebrick revealed that the WRe had burned its way through a portion of the firebrick near one of its edges. Due to this, another sample, (Nb-1%Zr) that had been near the WRe fell off of the firebrick. This was the sample that had become stuck to the ceramic tray. Additionally, it was determined that the C-103

sample had also burned through enough of the firebrick to fall off the brick. This sample was easily removed. The C-103 sample left a burn shaped in a circular ring on the surface of the firebrick, since the sample was originally a one inch length of one inch diameter pipe. There was significant evidence that the W-Re sample did not merely burn its way through the firebrick. Black burn marks on samples that neighbored the W-Re seem to indicate that the W-Re burned with an open flame before finally melting down the edge of the firebrick. As the W-Re melted its way down the side of the firebrick, a portion of it appears to have reacted with the aluminum in the firebrick to form a glass. The entire top edge of the firebrick, where the W-Re initially began burning through, had a layer of glass formed on it. It is still unclear whether the W-Re reacted alone to the temperature in the furnace, or whether the transformation was initiated by a chemical reaction between the W-Re and the firebrick.

W-Re was the only sample to deform to the point that oxidation on it could not be evaluated. The C-103 sample that fell off the firebrick was heavily oxidized. It appears that when the material fell, the impact of hitting the ceramic plate at the bottom of the furnace caused the oxide layer on the sample to fracture. It was unclear whether the Nb-1%Zr sample had oxidized. Apparently, since it fell due to the W-Re burning, some of the melted W-Re stuck to the Nb-1%Zr sample even after it had fallen off of the firebrick.

The MA956 was heavily oxidized. Further evaluation of the MA956 revealed that while there was heavy oxidation, the thick oxide coating was easily removed. Underneath, the MA956 seemed to have another oxide layer that was firmly fixed to the

surface of the sample. This oxide appeared black, which is a sign that it may have high emissivity, indicating the need for subsequent testing. The oxide appears as a dark gray pellet-like oxide that formed on the flat faces of the sample. The SiC sample did not appear to oxidize. The Si/SiC sample did not appear to have oxidized either, although burn marks were present on the edge that had been closest to the W-Re sample. The ZrO_2 and Al_2O_3 samples showed no sign of oxidation. The BN sample showed slight signs of oxidation although they were difficult to distinguish from the minor burns marks that resulted from the W-Re. The sputter coated BN sample showed no significant sign of oxidation.

The results of this experiment indicated that further testing was warranted. This testing is discussed in a subsequent section.

7.2 THERMAL SHOCK TESTING — PHASE I

Temperature conditions similar to those inside a T-58 gas turbine were emulated in order to measure the thermal shock response of candidate materials with suspect thermal shock resistances. This testing was designed as pass or fail such that if a material experienced cracking and/or catastrophic failure, it was eliminated from consideration as a suitable emitter or extraction tube material.

The thermal shock testing was conducted in the welding area of the U.S. Naval Academy Machine Shop. An acetylene torch with a maximum flame temperature between 1600-1800°C was used as the heat source. Four different material samples were

tested to evaluate response to thermal shock: Omegatite, zirconia, silicon carbide, and silicon carbide in a silicon matrix.

The Omegatite sample was a small cylindrical tube with a 0.5 inch outer diameter, 0.25 inch inner diameter, and 1 inch length. The sample was a very faint yellow before exposure to the flame. The zirconia was a cylindrical tube with 1 inch outer diameter, 0.5 inch inner diameter, and 12 inch length. The zirconia was initially a dull white color. The silicon carbide was a cylindrical tube measuring 1.5 inch outer diameter, 0.75 inch inner diameter, and 12 inches in length. It was a dark brownish gray prior to testing. The silicon carbide in a silicon matrix was a cylindrical tube measuring 2 inches in outer diameter, 1.75 inches in inner diameter, and a 2 inch length. Initially, it was dark gray with metallic-looking sparkles mixed into the outer surface.

The four samples were placed individually on a piece of firebrick and heated with the torch. The zirconia, silicon carbide, and silicon carbide in a silicon matrix samples were lightly constrained by additional pieces of firebrick that were pushed against the samples to prevent them from rolling under pressure from the flame. The torch was then used to heat a portion of each sample. The Omegatite was small enough that the acetylene torch flame heated the entire sample. In the case of the zirconia, the test did not last long enough to heat a significant portion of the sample. The silicon carbide was positioned such that a 2 inch portion hung over the side of the firebrick table; this two inch length was then evenly exposed to the flame. The silicon carbide in a silicon matrix sample was positioned on its side, while the opposite side of the cylinder was heated.

The Omegatite, which was initially a faint yellow, turned orange once exposed to the flame. After approximately 45 seconds, it became a luminous white. The sample did not fail catastrophically, but significant cracking did begin within 15 seconds of the flame being applied. While the sample did remain intact for the duration of the 3 minute test, it appeared cracked and weakened afterwards.

The zirconia sample was initially a dull white. When the flame from the blow torch was applied, the zirconia sample immediately shattered. The test lasted less than 1 second. Approximately 6 inches of the cylinder shattered even though the flame was directly applied only to one end of the cylinder. The scattered pieces were all jagged and indicated that catastrophic failure had resulted from rapid thermal expansion.

The silicon carbide sample remained a dull gray for the first minute of heating. Eventually the sample turned bright orange. The sample survived the entire 3 minute test and did not appear to experience any cracking. One small region at the end of the cylinder did melt after it was exposed to the direct flame for approximately 20 seconds, but the melting was not significant.

The silicon carbide in a silicon matrix gradually became a bright orange as it was heated. The sample survived the entire 3 minute test and did not show any significant cracking. At times, small cracks and pops were heard as the flame was moved to a new region of the cylinder, but the sounds most likely came from small imperfections (regions where the silicon carbide was not thoroughly mixed into the silicon matrix) that popped off of the inside of the cylinder. This did not hurt the structure of the silicon / silicon carbide since the imperfections were only on the surface.

Although the testing was qualitative rather than quantitative, it produced very significant results. Omegatite and zirconia were eliminated as candidate materials for both the emitter and the extraction tube. Zirconia had been considered for the extraction tube since published reports say that it is extremely resistant to thermal shock, but its thermal shock resistance does not extend to extreme temperatures. Omegatite is advertised as a high temperature thermal couple sheath material, but in a larger diameter it did not withstand thermal shock at the required temperatures. Silicon carbide performed very well under the extreme temperatures, but in order to work in current TPV design, a thinner walled cylinder would have to be used. The silicon / silicon carbide also performed very well under the conditions. Again, the silicon / silicon carbide would have to be made smaller in order to be used as the emitter or drawing tube. One inch diameters are available for the emitter, but finding a 0.5 inch diameter cylinder to serve as the extraction tube is more challenging. The findings are summarized in Table 3 below.

Table 3 Summary of Phase I Thermal Shock Test Results

Material	Results	Emitter?	Extraction Tube?	Concerns
Silicon Carbide	Turned bright orange	Yes	Yes	Availability in smaller diameters
Zirconia	Shattered	No	No	Catastrophic failure eliminates it
SiC/Si	Turned bright orange	Yes	Yes	Availability in smaller diameters
Omegatite	Turned luminous white Visible cracking	No	No	Catastrophic failure is possible

8.0 MATERIAL SELECTION

The process of high temperature material selection continued even after the initial materials had been ordered for testing. The initial materials that were ordered represented a survey of the available, commonly known high temperature materials. These materials were ordered early, so that samples would be available for testing. Additionally, it was better to develop testing techniques by experimenting on low cost materials, rather than waiting until further into the project to begin testing samples. It was understood that all or none of the materials initially examined might be selected as emitter materials. Additionally, those materials determined as unsuitable emitters may still find applications as structural components of the TPV assembly.

Material science and engineering is a rapidly growing industry. Due to this, many of the companies in the industry are small operations that advertise by word of mouth. Most of the time spent researching and searching for candidate materials was devoted to calling small companies by phone and searching the Internet for additional possibilities. Frequently, one company would pass on the name of another company that manufactured high temperature materials.

From the initial shock testing, it was evident that monolithic ceramics may be unable to withstand the temperatures and extreme environment of the TPV generator. Although thermal shock was primarily an issue with the extraction tube, the emitter is also exposed to a significant temperature gradient upon ignition. NASA Lewis Research Center suggested investigating ceramic matrix composites as a solution to the issue of thermal shock. There are numerous companies that specialize in manufacturing

composites. The task was to find companies that were involved more with researching new composites, rather than manufacturing and packaging standard composites, and that would be willing to tailor their work towards this project and its specific materials criteria.

After hours of phone calls, four companies were selected. INEX Incorporated was extremely interested in the project and was willing to provide free samples of their silicon carbide in a silicon matrix composite. The primary concern was that INEX Inc. did not manufacture the 0.5 inch outer diameter tubes required for the extraction tube. Additionally, the process that INEX Inc. uses requires extensive lead time to produce 1.0 inch outer diameter tubing.

Refractory Composites, Inc. (Glen Burnie, Maryland) provided a free sample of a 3-D carbon fiber in a silicon carbide matrix composite as well as information and recommendations on what materials should be used for specific applications.

Advanced Ceramics Research provided free samples of several of their composite materials. The samples included a silicon carbide fiber in a zirconia diboride / silicon carbide matrix composite, a zirconia diboride fiber in a boron nitride matrix composite, and a hafnium diboride fiber in a boron nitride matrix composite. The company also provided information and specifics on high temperature applications.

Ceramic Composites, Inc. is a local company that also provided free samples of composite materials. This company specializes in carbon fiber and silicon carbide fiber composites. Additionally, they have developed an original method of producing their composites rapidly, thus reducing costs. CCI provided free samples of their composite

materials and reviewed the ongoing TPV research so that they would be better able to suggest alternative composites.

The following table summarizes the composite samples that were obtained.

Table 4 Composite Samples Obtained

Material	Manufacturer	Sample Description
SiC/Si	INEX Incorporated	Tubing segments
C/SiC	Refractory Composites, Inc.	1" x 1" square piece
35 vol%SiC/ZrB ₂ -SiC	Advanced Ceramics Research	Segments
82.5/17.5 ZrB ₂ /BN	Advanced Ceramics Research	Segments
82.5/17.5 HfB ₂ /BN	Advanced Ceramics Research	Segments
C/SiC	CCI	Tubing segment
SiC/SiC	CCI	Tubing segment
SiC/SiC w/ SiC overcoat	CCI	Tubing segment
CVD SiC	CCI	1" x 1" square piece
CVD HfC	CCI	1.5" Diameter disk
HfC 4wt% TaC	CCI	Flat pieces
HfC 5wt% TaC	CCI	Flat pieces
HfC 7wt% TaC	CCI	Flat pieces
HfC 10wt% TaC	CCI	Flat pieces

9.0 PROPERTY VERIFICATION AND QUANTIFICATION

Once the initial testing was performed, and the field of candidate materials had been reduced, additional testing methods were developed to screen the remaining candidates further as well as some materials suggested by composites manufacturers. The initial oxidation experiment and thermal shock experiment had decisively eliminated many of the early candidate materials, such as tungsten-rhenium and zirconia. Some of the more advanced testing was conducted on a few of the initial candidate materials, even though they had already been eliminated from consideration. This was done for two reasons: to provide continuity to the research and to provide as much data about as many materials as possible.

9.1 OXIDATION EXPERIMENT — PHASE II

The purpose of the initial oxidation experiment was to evaluate general response of different candidate materials to a high temperature environment. From this test, two specific candidate materials were eliminated as possible emitter materials: C-103, and WRe. Additionally, questions were raised about MA956 and Nb-1%Zr. The purpose of the second oxidation experiment was to quantify the oxidation rates of the initial materials. Additionally, new candidate materials that had been selected after the initial testing was complete were tested to determine their respective oxidation rates.

The objective of this experiment was to expose the initial candidate materials to a high temperature free air environment in order to determine their corrosion rates as well as the corrosion rates of new candidate materials. The goal of this experiment was to

produce quantitative data for comparison of the corrosion resistance of the emitter candidates.

The following samples were tested:

Boron Nitride	C-103	MA956
Zirconia	Niobium-1%Zirconium	Tungsten-Rhenium
Silicon Nitride	Alumina	SiC/Si
ZrB ₂ /SiC	CVD SiC	CVD SiC/C
Woven C/SiC	CVD HfC	HfC-10%TaC
C/SiC with SiC		

The mass of each sample was first measured on a Sartorius digital scale. The Thermolyne furnace was next pre-heated to a temperature of 1315°C. Each sample was placed directly on a thin sheet of alumina, which was then placed in the furnace for a period of two hours. At the conclusion of each test, the sample was removed and allowed to cool to room temperature. When one sample was removed, the next sample was placed on an alumina sheet and placed in the furnace. After the heated sample had sufficiently cooled, its mass was again measured on the digital scale. Both the initial and final masses of each sample were recorded, and percent change was calculated.

As expected, boron nitride was the only initial material that actually lost significant mass while in the furnace. This loss of mass was due to sublimation as the material gradually decomposed into a gas. Most of the ceramic composites experienced mass loss due to fiber burn out because they did not have oxidation resistant coatings. Zirconia diboride in a silicon carbide matrix (ZrB₂/SiC) and CVD Silicon carbide in a carbon matrix (CVD SiC/C) were two samples that did not show significant mass change. Additionally, the carbon fiber in a silicon carbide matrix with silicon carbide overcoat (C/SiC w/ SiC) corroded on the inner diameter where there was no silicon carbide

overcoating, but did not corrode on the outside surface where the coating was present. The woven carbon in a silicon carbide matrix (Woven C/SiC) sample corroded because its light oxidation resistant coating did not cover all of its fibers, but a thicker coating would protect the sample.

Table 5 summarizes the results of the follow-on oxidation experiment:

Table 5 Summary of Phase II Oxidation Testing

Material	Initial Mass (grams)	Final Mass (grams)	Percent Mass Change	Observations
Boron Nitride	44.97	43.88	- 2.42%	Slight brown tint
C-103	30.05	34.72	+ 15.54%	Thick white oxide
MA956	90.82	91.80	+ 1.09%	Thick black oxide
Zirconia	28.23	28.22	- 0.04%	No change
Nb-1%Zr	111.27	113.24	+ 1.77%	Thick white oxide
W-Re	9.56	NA	NA	Vaporized, yellow residue remained
Silicon Nitride	44.77	44.82	+ 0.10%	Slightly darker gray
Alumina	1.49	1.49	0.00%	No noticeable change
SiC	113.47	112.98	-0.43%	No noticeable change
SiC/Si	10.64	10.65	+0.09%	Slightly darker gray
ZrB ₂ /SiC	18.60	18.71	+0.59%	Surface became semi-reflective gray
CVD SiC	6.85	3.04	-55.62%	Thick white oxide - hollow inside
CVD SiC/C	4.82	4.83	+0.21%	No noticeable change
Woven C/SiC	7.74	6.18	-20.16%	Fibers exposed on surface
CVD HfC	9.48	3.32	-64.98%	Thick white oxide - hollow inside
HfC-10%TaC	4.48	3.14	-29.91%	Thick white oxide - hollow inside
C/SiC w/ SiC	1.33	1.02	-23.31%	Non-coated inside diameter oxidized

9.2 THERMAL SHOCK TESTING - PHASE II

The second thermal shock test was conducted at the facilities of Technology Assessment & Transfer, Inc. in Annapolis, MD. The initial testing which had been conducted in the United States Naval Academy's machine shop had been a pass/fail test designed to survey candidate materials and eliminate any materials that catastrophically failed on heating.

The purpose of the second test was to qualitatively compare the response of a wide range of candidate materials to thermal shock. In order to compare the candidate materials, a pyrometer was used to ensure that all samples were heated to the same temperature by an acetylene torch. Thermal shock upon heating was visually observed once the acetylene torch was focused on the sample. Thermal shock upon cooling was observed by quenching the candidate materials in air and water.

Two identical samples of each material were first cut. The materials tested were:

Boron Nitride	C-103	MA956
Niobium-1%Zirconia	Silicon Carbide	SiC/Si
Tungsten-Rhenium	Zirconia	Alumina
C/SiC w/ SiC	ZrB ₂ /SiC	Woven C/SiC
CVD SiC/C	Silicon Nitride	

The materials were placed on pieces of alumina panels which were laid across a grill. An acetylene torch was used to heat one of the samples as shown in Figure 14. During the heating, an optical pyrometer was focused on the sample. The optical pyrometer was pre-set to



Figure 14 Acetylene torch and pyrometer

indicate a temperature of 1315°C . When the color of the sample being heated matched the color of the pre-set filament inside of the pyrometer, the temperature of the sample had reached 1315°C . Once this temperature was achieved, the hot sample was picked up with tongs and quenched in a bucket of room temperature tap water as shown in Figure 15.

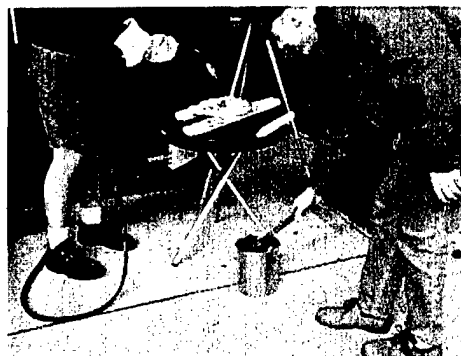


Figure 15 Water quenching

The acetylene torch was next directed at the second identical sample. This sample was again heated to a temperature of 1315°C . Once this sample reached the specified temperature, the acetylene torch was removed and the sample was allowed to quench in the open air. Once the samples had both cooled, they were placed side by side, compared, and photographed.

The following details the results of the thermal shock experiment for each candidate material:

Boron Nitride

Boron nitride demonstrated an excellent resistance to thermal shock. Neither sample appeared affected by the initial heat-up when the acetylene torch was applied. Upon quenching, the water quenched sample turned black in the areas that the acetylene torch had been applied. The air-cooled

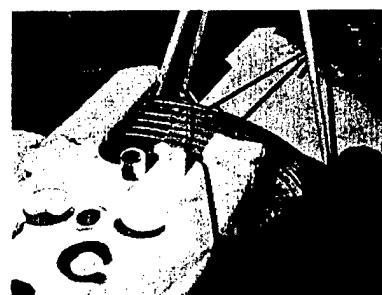


Figure 16 Shock tested Boron Nitride

sample had several regions where a light brown coating had developed, but not to the extent of the black coating on the water quenched sample as shown in Figure 16.

C-103

The C-103 samples demonstrated thermal shock resistance upon heating. Both samples quickly formed thick white oxide layers on both the inside and outside of the cylinder as seen in Figure 17. When the first sample was water quenched, the oxide layer fractured and fell off

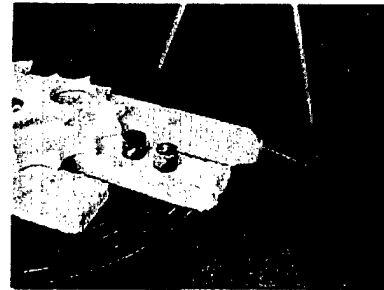


Figure 17 Shock tested C-103

of the sample. When the second sample was air quenched, flakes of the oxide layer began blowing off in the wind, although more of the oxide remained on the air quenched sample than remained on the water quenched sample.

MA956

As expected with most metals, MA956 exhibited no thermal shock problems upon initial heating. Gradually, however, a dark oxide layer formed on the outside of both samples. When the first sample was water quenched, the oxide coating fractured and fell off of the sample. The MA956 metal which was exposed when the oxide coating fell off appeared slightly darker than the non-oxidized sample. The thick



Figure 18 Shock tested MA956

dark gray oxide coating did not fall off of the air quenched sample as seen in Figure 18.

Nb-1%Zr

The Nb-1%Zr samples did not demonstrate any adverse response to the thermal shock caused upon heating. Like many of the other metal alloys, Nb-1%Zr developed an oxide layer during heating. The oxide coating on the water quenched sample became a dark gray upon cooling, while the oxide coating on the air quenched sample remained white in color as seen in Figure 19. Neither sample demonstrated difficulties with thermal shock due to cooling.

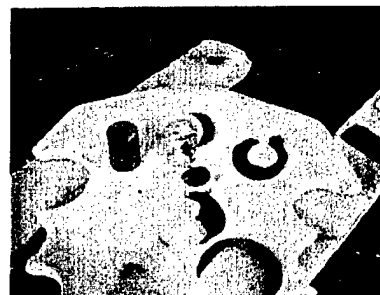


Figure 19 Shock tested Nb-1%Zr

Silicon Carbide

The silicon carbide samples did not fail catastrophically from the thermal shock caused by the initial heating, but cracking did propagate within the matrix. The cracking was noticeable because the color of the cracking regions contrasted the orange glow of the rest of the sample at 1315°C. A light oxide coating formed on the outside of the samples during heating. Water quenching caused the oxide on the sample to turn a darker gray than the oxide on the air quenched sample as seen in Figure 20. The oxide layer did not crack from quenching.



Figure 20 Shock tested SiC

Silicon Carbide in a Silicon Matrix

The SiC/Si samples were not affected by thermal shock due to heating. Light oxide layers gradually formed on the samples however. When the first sample was water quenched, the oxide layer rapidly transformed into a dark gray layer. The air quenched sample's oxide layer remained white in color as seen in Figure 21. Neither oxide layer fractured due to thermal shock caused by cooling.

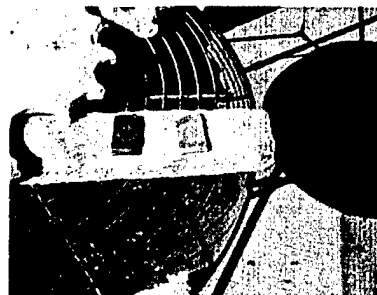


Figure 21 Shock tested SiC/Si

Tungsten-Rhenium

Neither sample of tungsten-rhenium demonstrated any problems with thermal shock due to heat-up. Both samples oxidized from the heating, and left a yellowish rhenium residue on the alumina, when the samples were removed as seen in Figure 22. Neither the water quenched nor air quenched samples appeared to experience adverse effects from thermal shock due to cool down.



Figure 22 Shock tested W-Re

Zirconia

The zirconia samples did not survive initial heating. The first sample fractured immediately when the acetylene torch was directed towards it as seen in Figure 23. A second sample was not heated, and the samples were not quenched, since the samples would never survive the heating cycle.



Figure 23 Shock tested Zirconia

Alumina

The alumina sample demonstrated excellent thermal shock resistance upon heating. The sample was not affected by air quenching. Water quenching caused the sample to fracture down the length of the sample, creating two wafer thin pieces, as seen in Figure 24.

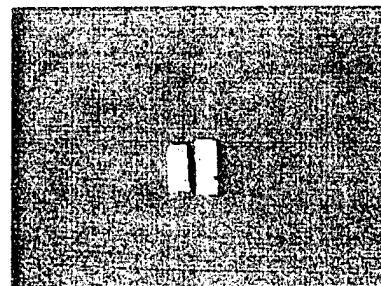


Figure 24 Fractured Alumina Sample

C/SiC with SiC Overcoat

The carbon fiber / silicon carbide matrix with silicon carbide overcoat sample demonstrated a resistance to thermal shock upon heating. The sample also withstood air quenching. Water quenching caused the inner diameter layer that had

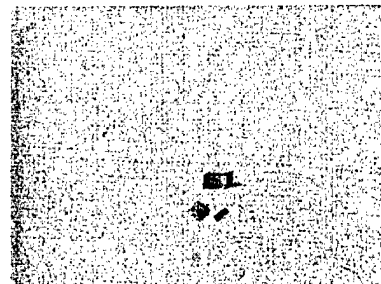


Figure 25 Shock Tested C/SiC w/ SiC

oxidized to separate from the rest of the sample, as seen in Figure 25. This reveals that the C/SiC composite by itself does not withstand thermal shock after it has been oxidized. In this application the C/SiC would be made with both an inner and outer SiC coating, so thermal shock is be of minimal concern since the oxidized layer is never given the opportunity to form.

Zirconia Diboride in a Silicon Carbide (ZrB_2/SiC)

Zirconia Diboride in a Silicon Carbide demonstrated excellent thermal shock resistance. The sample did not show any evidence of being affected by heating, air quenching, or water quenching as seen in Figure 26.

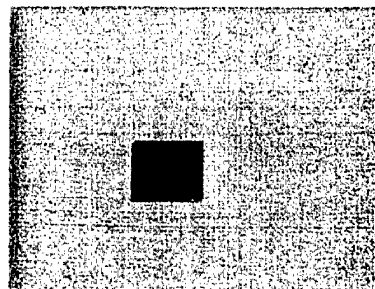


Figure 26 Shock Tested ZrB_2/SiC

Woven C/SiC

The sample of woven carbon in a silicon carbide, seen in Figure 27, was not affected by thermal shock upon heating or cooling. Air quenching and water quenching had little influence on the sample.

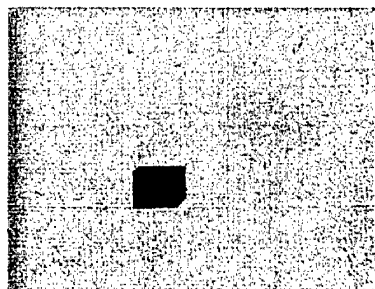


Figure 27 Shock Tested Woven C/SiC

CVD SiC/C

CVD Silicon Carbide in a Carbon Matrix, as seen in Figure 28, was not significantly affected by thermal shock. After heating, air quenching and water quenching did not affect the sample.

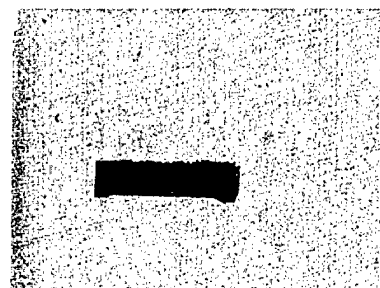


Figure 28 Shock Tested CVD SiC/C

Silicon Nitride

Silicon Nitride did not exhibit any adverse effects induced by thermal shock. The sample withstood air quenching and water quenching after being heated above 1300°C, as seen in Figure 29.

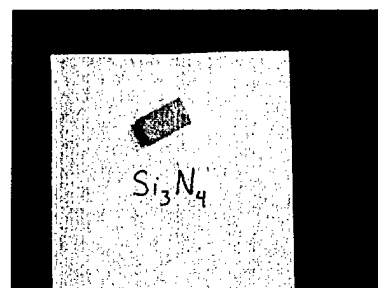


Figure 29 Shock Tested Silicon Nitride

Table 6 summarizes the results of the Phase II Thermal Shock experiments.

Table 6 Phase II Thermal Shock Results

Material	Observations
BN	Excellent shock resistance. Water quenching turned surface black
C-103	White oxide formed which fractured upon quenching
MA956	Dark oxide formed which fractured upon quenching
Nb-1%Zr	Light oxide formed became dark gray upon water quenching
SiC	Cracks visible during heating, but no failure
SiC/Si	White oxide formed, turned dark gray after water quenching
WRe	Yellow residue
Zirconia	Shattered
Alumina	Sample split lengthwise from thermal shock when water quenched
C/SiC w/ SiC	Oxidized inner layers fractured when water quenched
ZrB ₂ /SiC	No visible effects
Woven C/SiC	No visible effects
CVD SiC/C	No visible effects
Silicon Nitride	No visible effects

9.3 EMISSIVITY TESTING

Emissivity testing was conducted at NASA Lewis Research Center in Cleveland, Ohio. A wide range of samples was tested, including some new composite materials that had not been initially selected as candidate materials. Composite materials with oxidation resistant coatings emerged as emitter material candidates due to their excellent thermal shock resistance, characteristically high emissivities, and greater toughness than

monolithic ceramics. Ceramic composites were tested for their emissivities to verify published reports.

The objective of the emissivity testing was to obtain emissivity data for a wide range of emitter candidate materials including refractory metals, monolithic ceramics, and composite ceramics. Emissivity is one of the critical parameters for the emitter material, but it is also the one material property that has the least published data available.

The individual samples were first placed in the detector's sample holder, seen in Figure 30. The detector was a

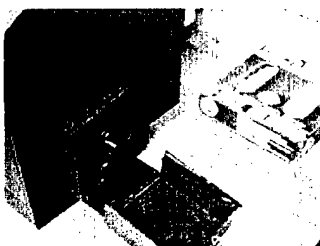


Figure 30 Sample Holder

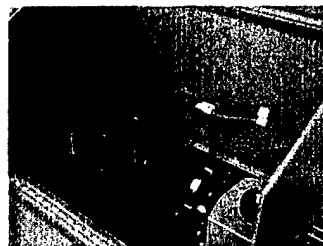


Figure 31 Emissivity Measuring System

large black box that contained a system of mirrors, lamps, and an integrator, as seen in Figure 31. Essentially, a series of lamps and filters were used to selectively radiate the samples with light of a specific wavelength. A system of mirrors was then used to capture the light that was reflected from the samples surface. This light was directed to an integrator that calculated the reflectivity. A plot of the sample's reflectivity versus wavelength was displayed on a nearby monitor that was connected to the system, as shown in Figure 32

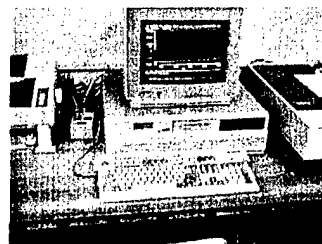


Figure 32 Computer Display

Figure 32. The data used to generate the plots were saved, and correction factors were applied to account for the fact that the atmosphere within the test chamber was not a

vacuum and that the test was conducted at room temperature. The material's emittance was extrapolated and plotted as a function of the incident wavelength and corresponding temperature [19,20].

The data were organized into two formats. A table was created to list the emittance of a particular material for a range of temperatures (300K–1500K). Subsequently, a plot was generated from this data. The data and plots for the materials tested follow.

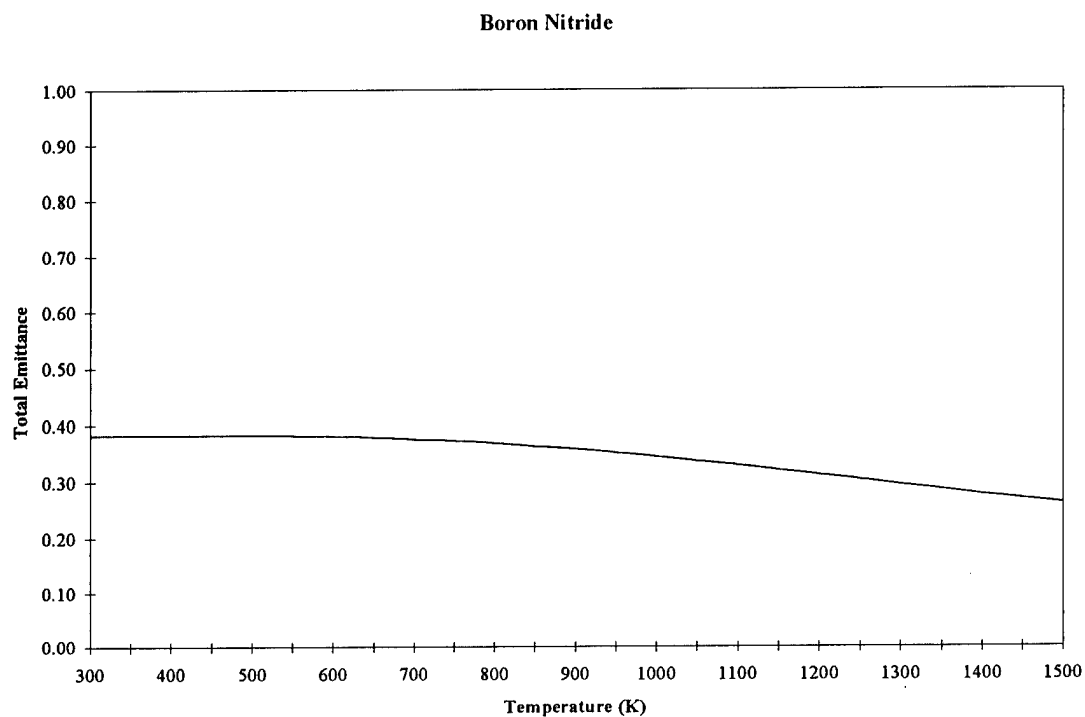


Figure 33 Emissivity of Boron Nitride

Boron nitride was one of the few initial candidate materials tested for emissivity. BN failed the oxidation testing, but so little data was published on boron nitride emissivity that the test was conducted for general knowledge. BN had an emissivity of 0.26 at 1500K. This low emissivity further eliminated BN as an emitter material candidate.

Table 7 Emissivity of BN

Boron Nitride	
Temperature (K)	Emissivity
300	0.38
400	0.38
500	0.38
600	0.38
700	0.38
800	0.37
900	0.36
1000	0.34
1100	0.33
1200	0.31
1300	0.30
1400	0.28
1500	0.26

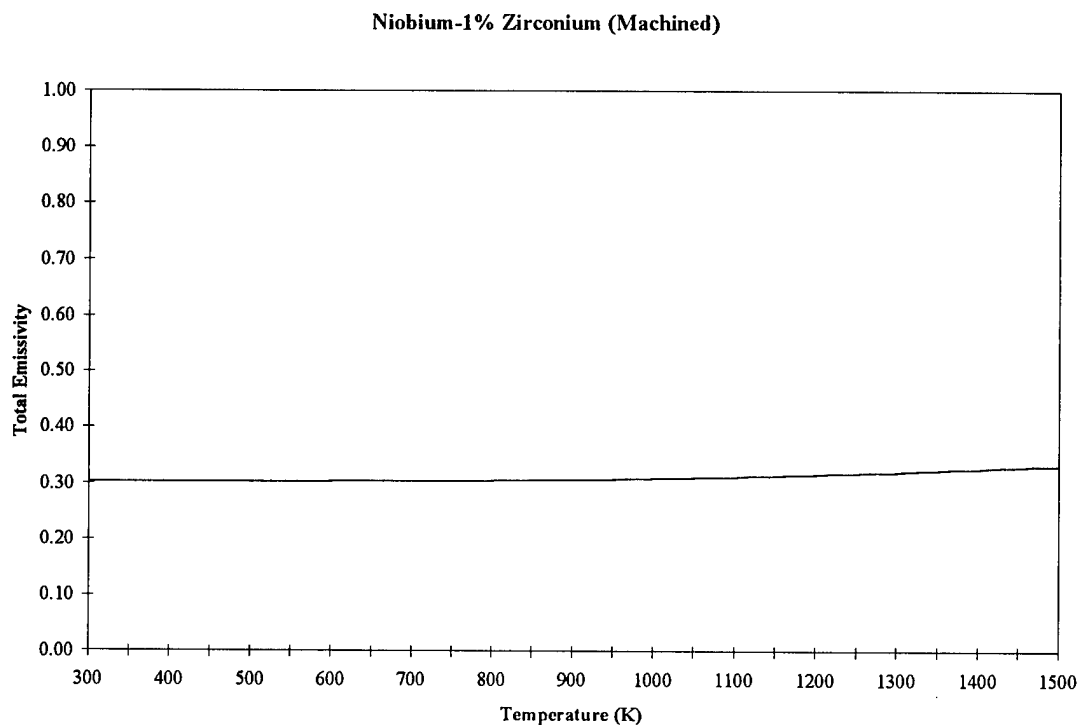


Figure 34 Emissivity of Nb-1%Zr

Niobium-1% Zirconium fell short of the targeted emissivity, registering a peak of 0.33 at a temperature of 1500K. Due to the configuration of the sample, this emissivity was measured from the machined end of a one inch rod sample. Most likely, the surface texturing due to the machining (caused when cutting the sample) raised the emissivity of the sample above that of a smooth sample.

Table 8 Emissivity of Nb-1%Zr

Niobium w/ 1% Zirconium	
Temperature (K)	Emissivity
300	0.30
400	0.30
500	0.30
600	0.30
700	0.30
800	0.30
900	0.31
1000	0.31
1100	0.31
1200	0.32
1300	0.32
1400	0.33
1500	0.33

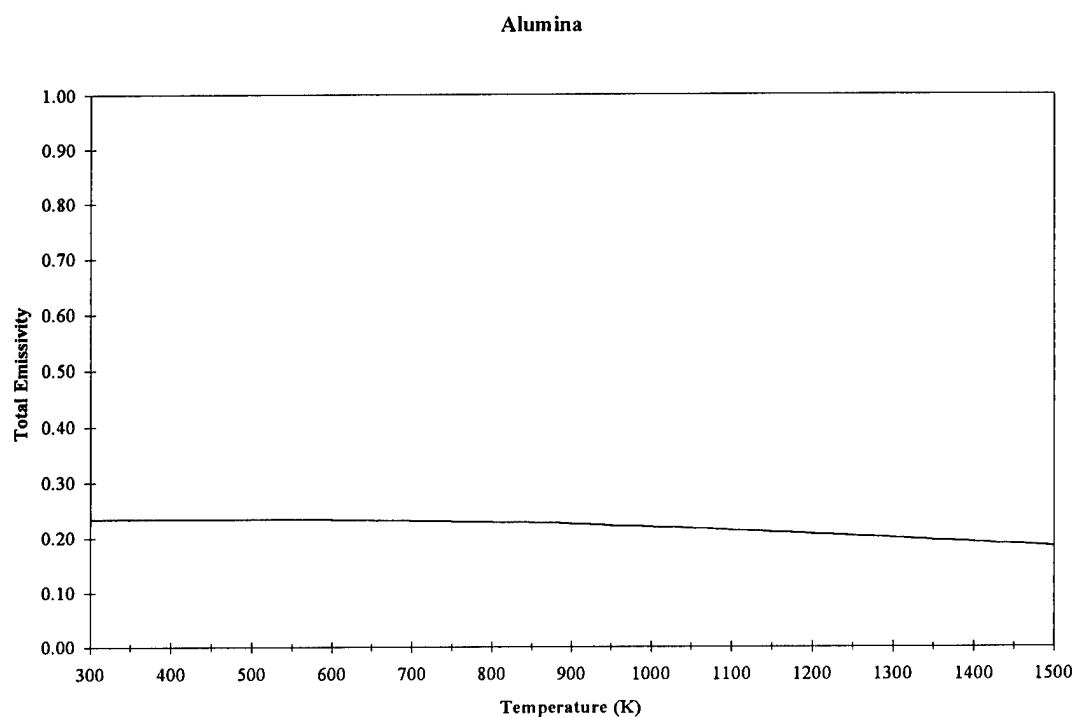


Figure 35 Emissivity of Alumina

Alumina did not reach the targeted emissivity, registering a peak of 0.23. The emissivity fell to 0.18 at a temperature of 1500K. This data further eliminated alumina from consideration.

Table 9 Emissivity of Alumina

Alumina	
Temperature (K)	Emissivity
300	0.23
400	0.23
500	0.23
600	0.23
700	0.23
800	0.23
900	0.22
1000	0.22
1100	0.21
1200	0.21
1300	0.20
1400	0.19
1500	0.18

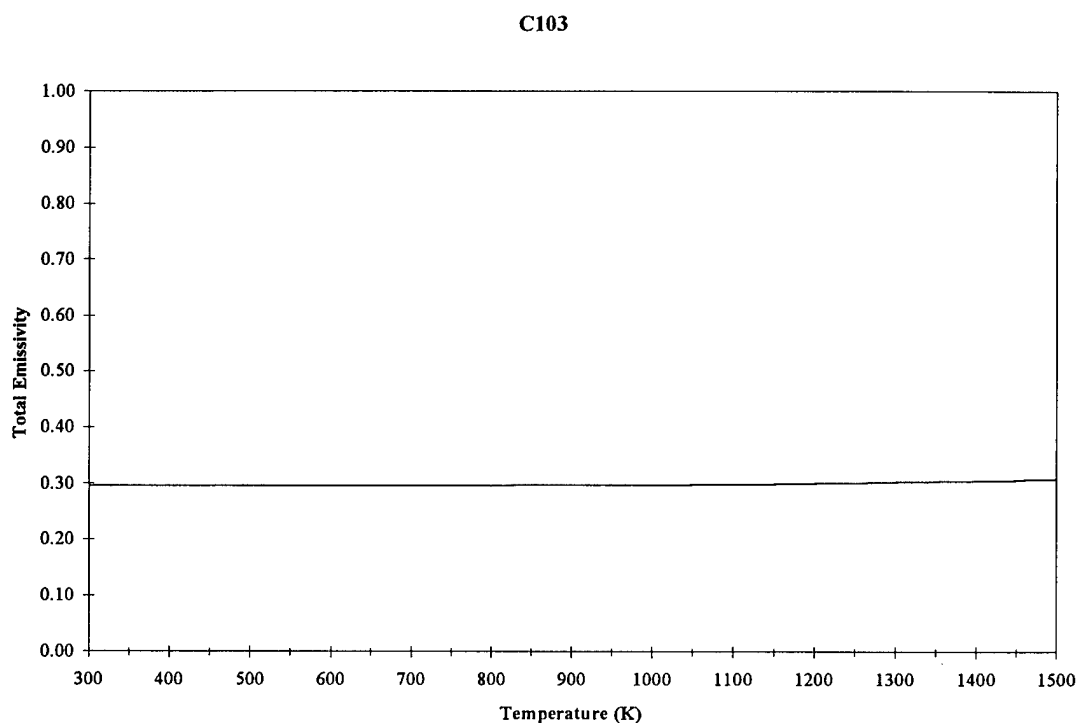


Figure 36 Emissivity of C-103

C-103 did not achieve the necessary emissivity for an emitter material. The peak emissivity of 0.31 occurred at 1500K. This sample's emissivity was difficult to measure due to the curved shiny surface of the sample.

Table 10 Emissivity of C-103

C-103	
Temperature (K)	Emissivity
300	0.30
400	0.30
500	0.30
600	0.30
700	0.30
800	0.30
900	0.30
1000	0.30
1100	0.30
1200	0.30
1300	0.30
1400	0.30
1500	0.31

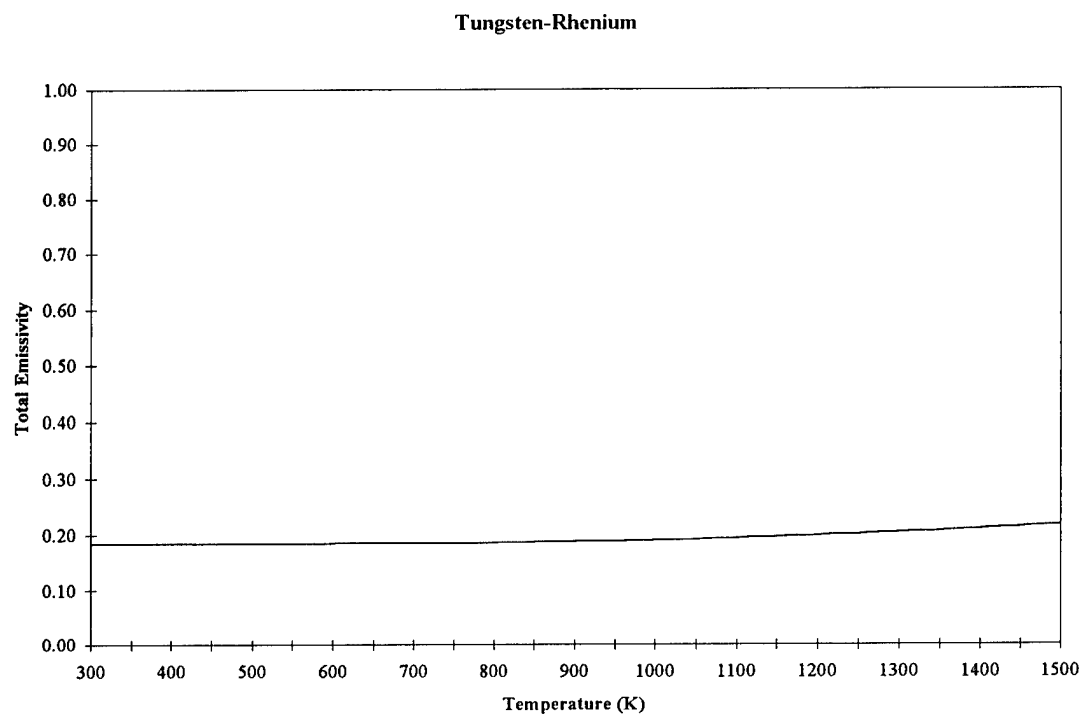


Figure 37 Emissivity of WRe

Tungsten-40%Rhenium's emissivity was very low as compared to the required value for an emitter material. Given its poor performance in the oxidation test, the emissivity results eliminated Tungsten-40%Rhenium as a potential emitter material.

Table 11 Emissivity of WRe

Tungsten-40%Rhenium	
Temperature (K)	Emissivity
300	0.18
400	0.18
500	0.18
600	0.18
700	0.18
800	0.19
900	0.19
1000	0.19
1100	0.19
1200	0.20
1300	0.20
1400	0.21
1500	0.22

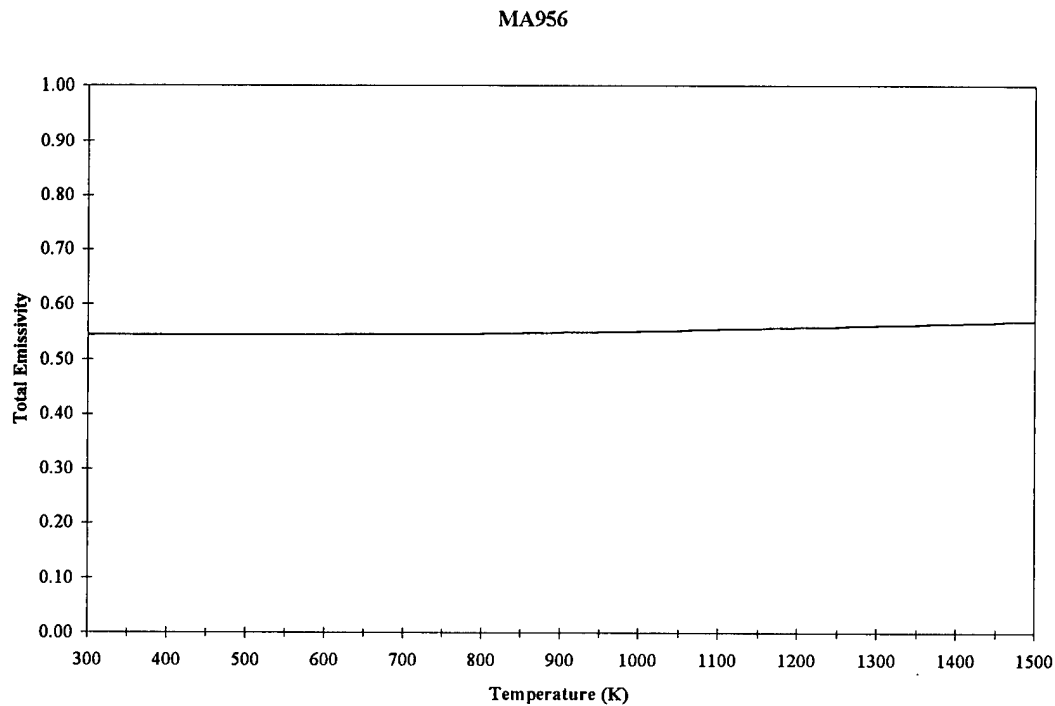


Figure 38 Emissivity of MA956

MA956 did not satisfy the emissivity requirements for the TPV emitter. The peak emissivity of 0.57 occurred at 1500K. Emissivity for MA956 was relatively constant across the entire temperature range tested.

Table 12 Emissivity of MA956

MA956	
Temperature (K)	Emissivity
300	0.54
400	0.54
500	0.54
600	0.55
700	0.55
800	0.55
900	0.55
1000	0.55
1100	0.55
1200	0.56
1300	0.56
1400	0.57
1500	0.57

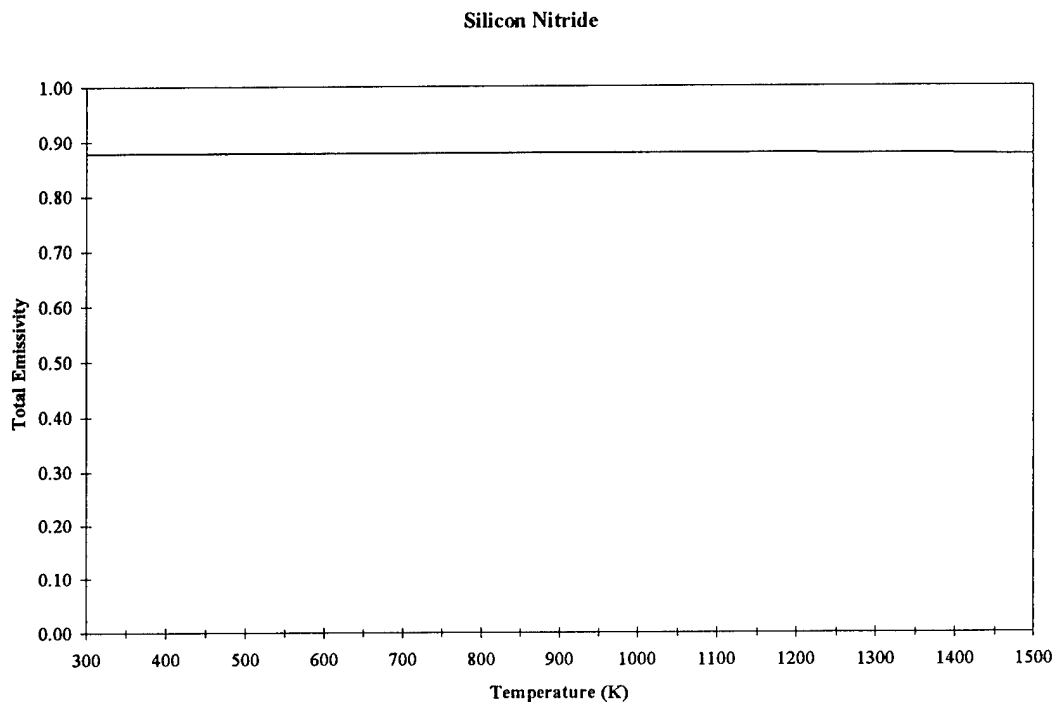


Figure 39 Emissivity of Silicon Nitride

Silicon nitride's emissivity was high, reaching 0.88 at most temperatures. At 1500K the emissivity dropped slightly to 0.87. These results indicate that ceramic composites containing silicon nitride will have similarly high emissivities.

Table 13 Emissivity of Silicon Carbide

Silicon Nitride	
Temperature (K)	Emissivity
300	0.88
400	0.88
500	0.88
600	0.88
700	0.88
800	0.88
900	0.88
1000	0.88
1100	0.88
1200	0.88
1300	0.88
1400	0.88
1500	0.87

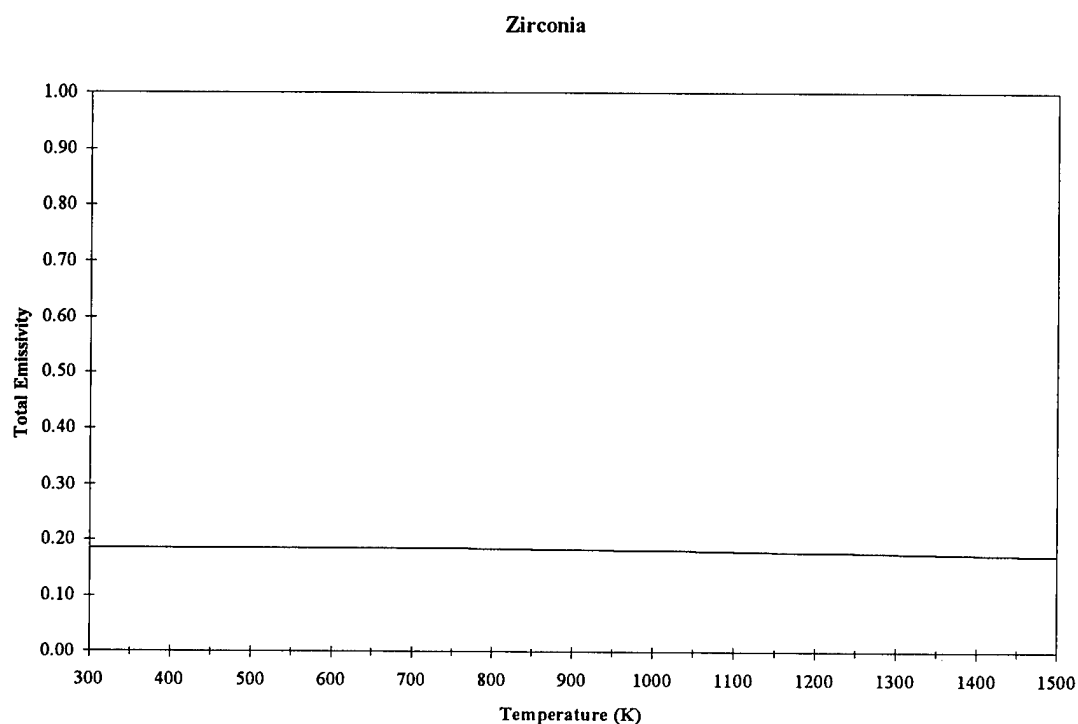


Figure 40 Emissivity of Zirconia

Zirconia demonstrated extremely low emissivity, ranging between 0.17 and 0.19. This material will not satisfy the requirements of a TPV emitter.

Table 14 Emissivity of Zirconia

Zirconia	
Temperature (K)	Emissivity
300	0.19
400	0.19
500	0.19
600	0.19
700	0.19
800	0.18
900	0.18
1000	0.18
1100	0.18
1200	0.18
1300	0.18
1400	0.17
1500	0.17

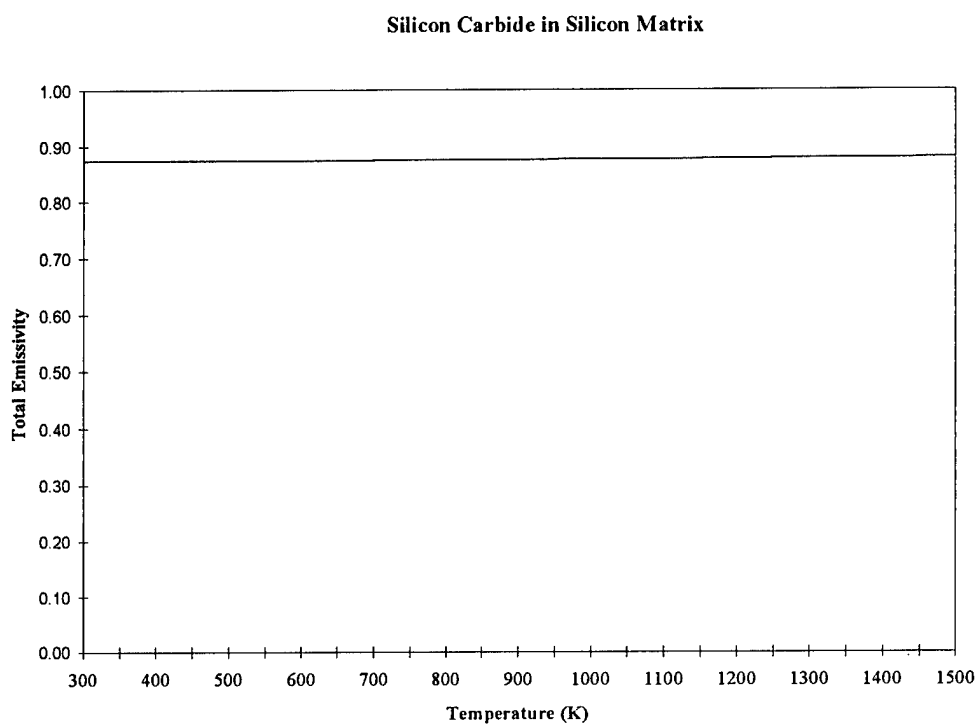


Figure 41 Emissivity of SiC/Si

SiC/Si appears to be a potential emitter material according to this data. Although its emissivity of 0.88 at 1500K is slightly below the goal of 0.90, SiC/Si can be used in trials until a better material is found.

Table 15 Emissivity of SiC/Si

SiC/Si	
Temperature (K)	Emissivity
300	0.87
400	0.87
500	0.87
600	0.87
700	0.87
800	0.87
900	0.87
1000	0.88
1100	0.88
1200	0.88
1300	0.88
1400	0.88
1500	0.88

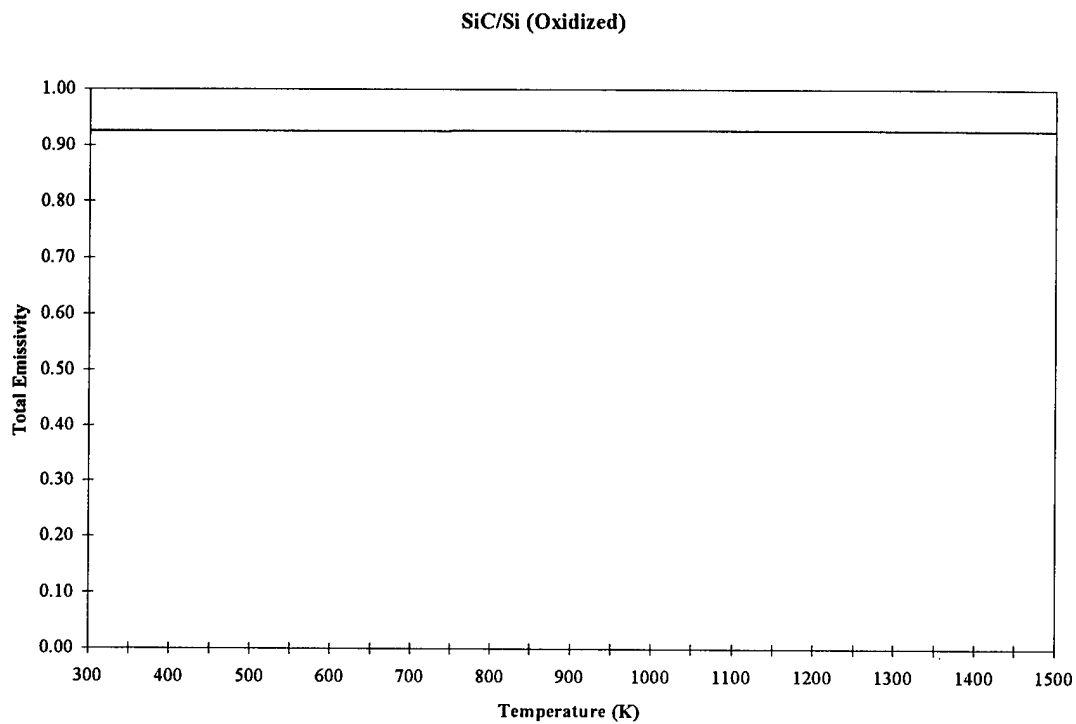


Figure 42 Emissivity of Oxidized SiC/Si

The emissivity results of oxidized SiC/Si further confirmed the material as a potential emitter. The thin oxide layer that developed on the surface of the material in the Thermolyne furnace caused the emissivity of the sample to rise from 0.88 to 0.93 at 1500K.

Table 16 Emissivity of Oxidized SiC/Si

Oxidized SiC/Si	
Temperature (K)	Emissivity
300	0.93
400	0.93
500	0.93
600	0.93
700	0.93
800	0.93
900	0.93
1000	0.93
1100	0.93
1200	0.93
1300	0.93
1400	0.93
1500	0.93

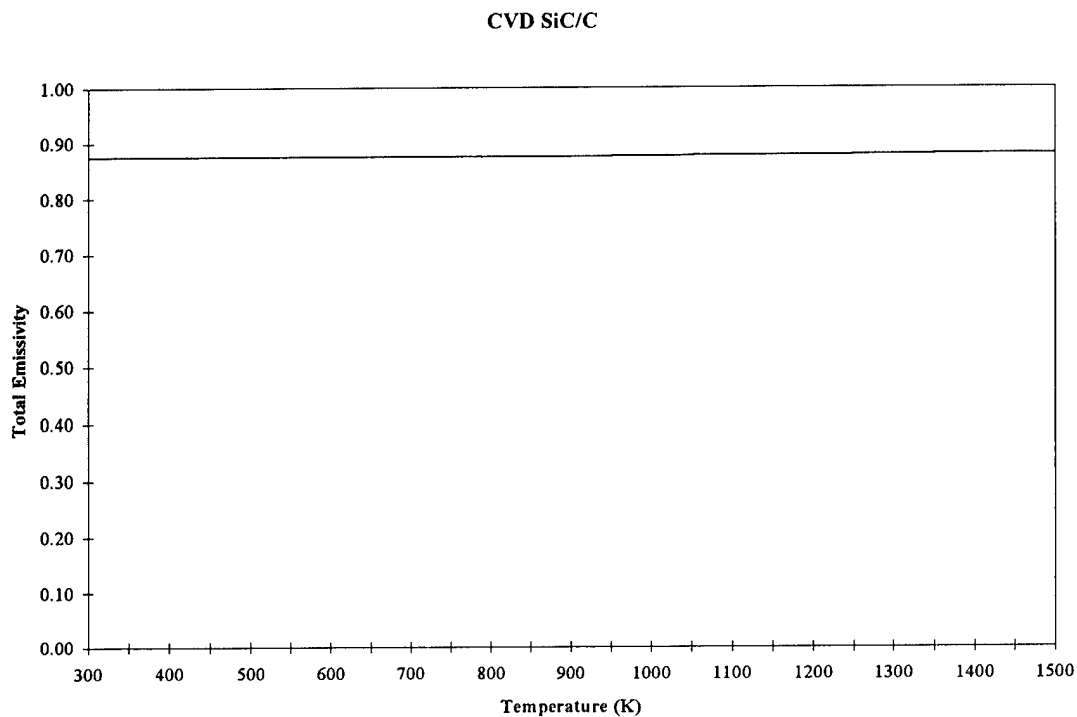


Figure 43 Emissivity of CVD SiC/C

CVD SiC/C exhibited promising emissivity results of 0.88 at 1500K. While this result is still below the goal, results indicated that silicon carbide fiber composite matrices exhibit high emissivities.

Table 17 Emissivity of CVD SiC/C

CVD SiC/C	
Temperature (K)	Emissivity
300	0.87
400	0.87
500	0.87
600	0.87
700	0.87
800	0.88
900	0.88
1000	0.88
1100	0.88
1200	0.88
1300	0.88
1400	0.88
1500	0.88

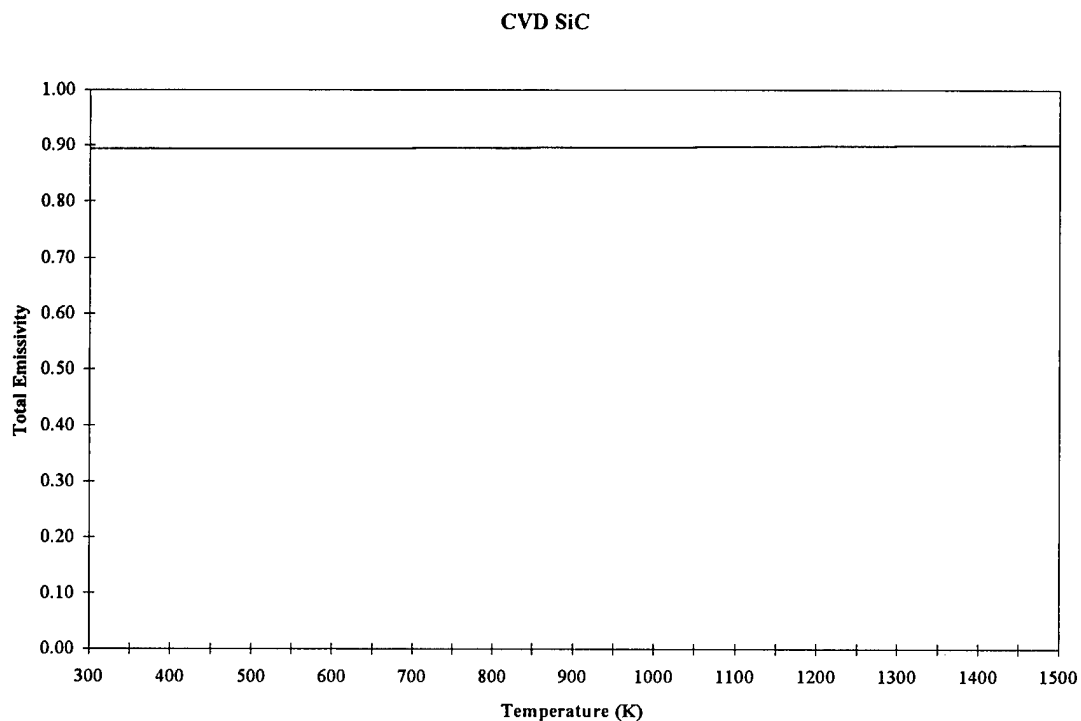


Figure 44 Emissivity of CVD SiC

CVD SiC possessed an emissivity of 0.90 at 1500K. CVD SiC is typically a coating applied to Woven fiber composite ceramics. Since emissivity is a surface phenomenon, this coating enables any woven composite to obtain the required emissivity of 0.90.

Table 18 Emissivity of CVD SiC

CVD SiC	
Temperature (K)	Emissivity
300	0.89
400	0.89
500	0.89
600	0.89
700	0.89
800	0.89
900	0.90
1000	0.90
1100	0.90
1200	0.90
1300	0.90
1400	0.90
1500	0.90

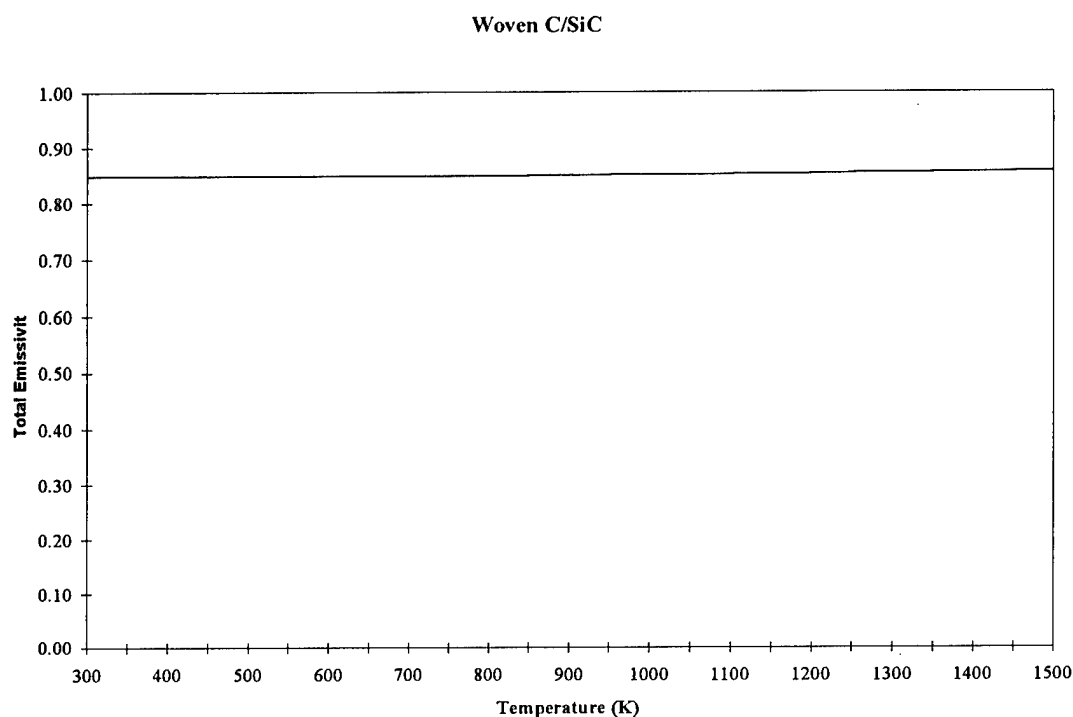


Figure 45 Emissivity of Woven C/SiC

Woven C/SiC was the only woven composite tested for emissivity. This test was conducted to establish a baseline from which woven composite emissivities may be estimated. This particular composite had an emissivity of 0.86 at 1500K, and lower emissivities at lower temperatures. For this application, a woven composite needs an overcoat to provide oxidation resistance. It is this coating that determines the emissivity of the composite piece.

Table 19 Emissivity of Woven C/SiC

Woven C/SiC	
Temperature (K)	Emissivity
300	0.85
400	0.85
500	0.85
600	0.85
700	0.85
800	0.85
900	0.85
1000	0.85
1100	0.85
1200	0.85
1300	0.85
1400	0.86
1500	0.86

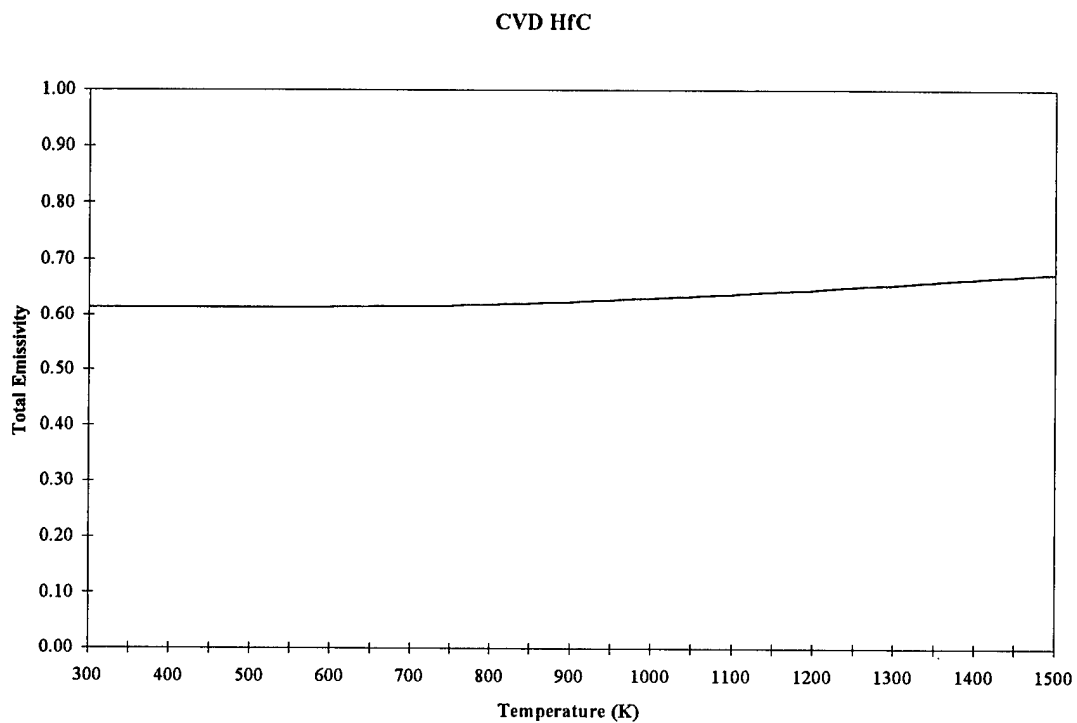


Figure 46 Emissivity of CVD HfC

CVD HfC is a common high temperature oxidation resistant coating, but it does not have a high emissivity relative to other oxidation resistant coatings. At 1500K, CVD HfC had an emissivity of only 0.67 which falls short of the stated goal.

Table 20 Emissivity of CVD HfC

CVD HfC	
Temperature (K)	Emissivity
300	0.61
400	0.61
500	0.61
600	0.61
700	0.62
800	0.62
900	0.62
1000	0.63
1100	0.64
1200	0.65
1300	0.66
1400	0.66
1500	0.67

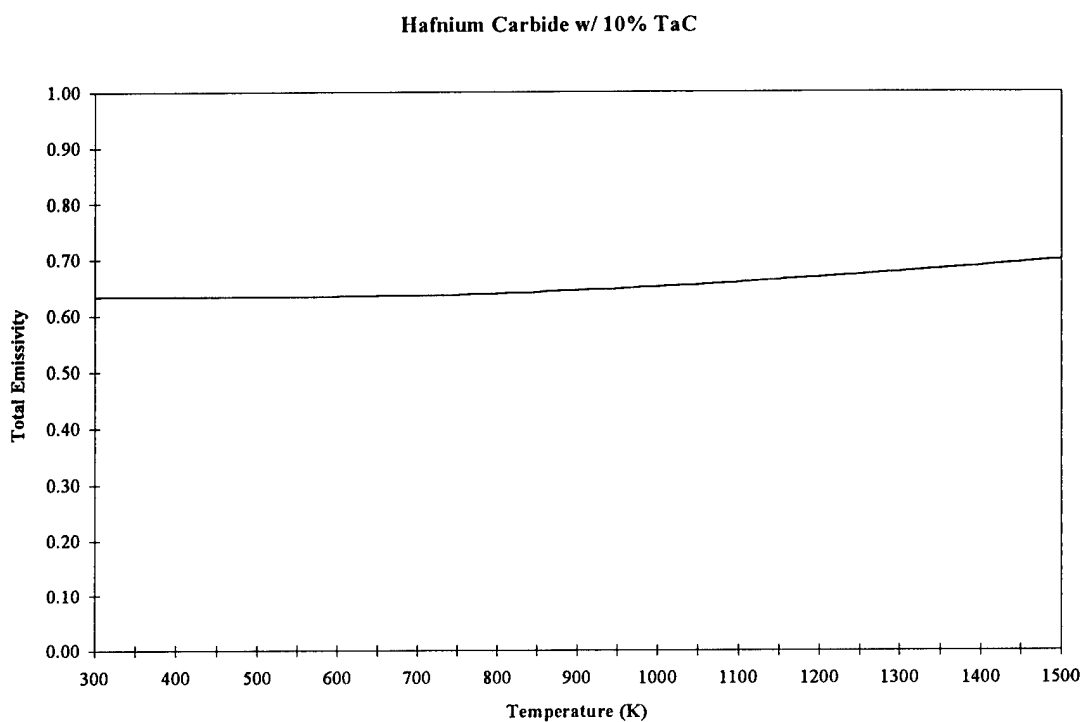


Figure 47 Emissivity of HfC - 10%TaC

HfC-10%TaC showed emissivities similar to CVD HfC. The Tantalum Carbide does not appear to significantly influence the emissivity of the material. The emissivity of HfC-10%TaC was only 0.03 higher than for CVD HfC. Since TaC influence was subtle, additional samples that contained higher weight percentages of Tantalum Carbide were not tested.

Table 21 Emissivity of HfC-10%TaC

HfC-10%TaC	
Temperature (K)	Emissivity
300	0.63
400	0.63
500	0.63
600	0.63
700	0.64
800	0.64
900	0.64
1000	0.65
1100	0.66
1200	0.67
1300	0.68
1400	0.69
1500	0.70

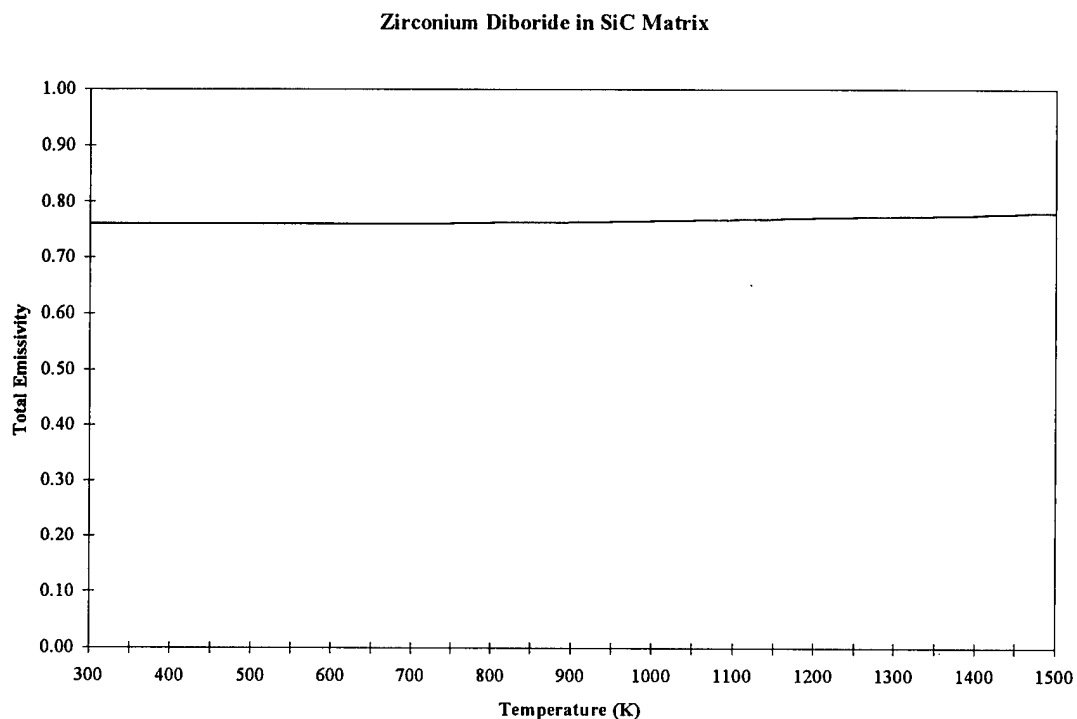


Figure 48 Emissivity of ZrB_2/SiC

Zirconia Diboride fibers in a Silicon Carbide Matrix exhibited an emissivity of 0.78 at 1500K. This composite material falls short of meeting the requirements for an emitter material.

Table 22 Emissivity of ZrB_2/SiC

Zirconium Diboride/SiC	
Temperature (K)	Emissivity
300	0.76
400	0.76
500	0.76
600	0.76
700	0.76
800	0.76
900	0.76
1000	0.77
1100	0.77
1200	0.77
1300	0.77
1400	0.78
1500	0.78

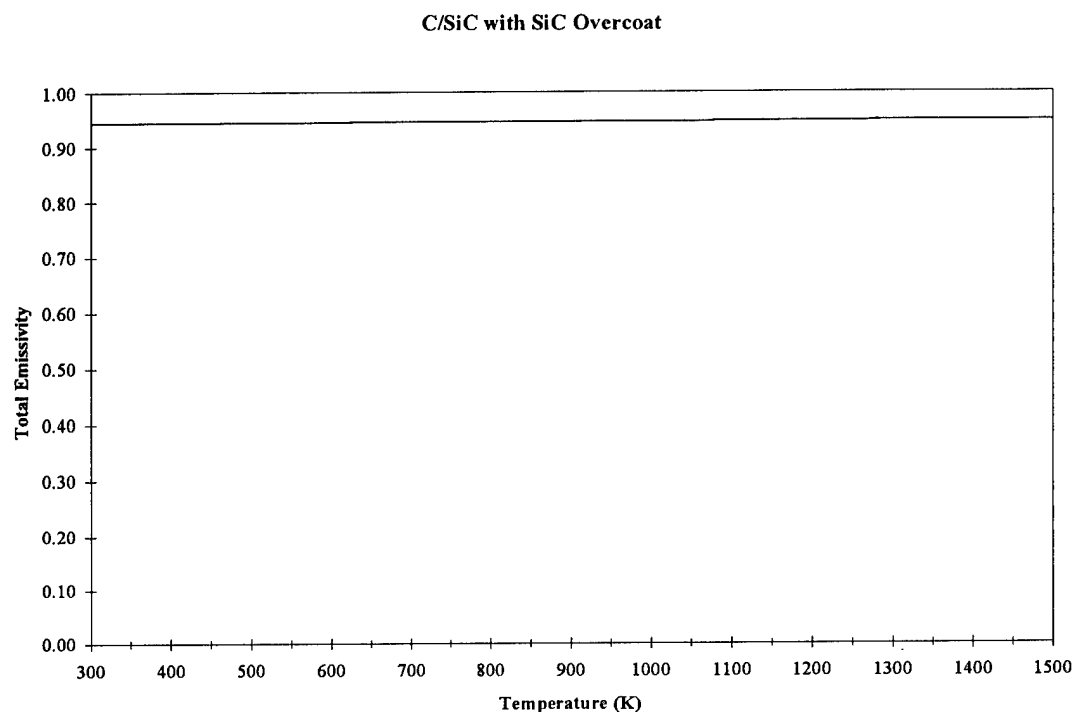


Figure 49 Emissivity of C/SiC w/ SiC

A composite made from carbon fiber within a silicon carbide matrix with a silicon carbide overcoat demonstrated promising emissivity. The emissivity results establish this material as the best emitting material of all the candidates, with a value of 0.95 at all temperatures.

Table 23 Emissivity of C/SiC w/ SiC

C/SiC w/ SiC	
Temperature	Emissivity
300	0.95
400	0.95
500	0.95
600	0.95
700	0.95
800	0.95
900	0.95
1000	0.95
1100	0.95
1200	0.95
1300	0.95
1400	0.95
1500	0.95

10.0 FINAL MATERIAL SELECTION

The final material selection was based on material research and testing. The results of the experiments conducted and the data obtained from the published literature as well as manufacturer's data for each material were weighted based on their significance.

10.1 MATERIAL PROPERTIES

The table on the next page summarizes the material properties of the candidate materials tested. Table 24 combines the results from each of the individual tests that were detailed in the preceding sections.

Table 24 Summary of Candidate Material Properties

Manufacturer	Melting Temperature C	Thermal Shock Resistance @ 1300C	Emmissivity 0.00 - 1.00	Oxidation Resistance @ 1300C	Machinability	Thermal Conductivity W/m-K	Thermal Expansion um/mK
Alumina	12	>1315	0.18	Excellent	Poor	29	5
BN	6	>1315	0.26	Excellent	Excellent	<0.6@500C	0.6
C-103	5	>1315	0.31	Poor (oxide)	Fair	41.9	8.1
CVD HfC	1	>1315	0.67	Excellent	Fair	0.05 - 0.40	1 - 10
C/SiC w/ SiC Overcoat	1	>1315	0.95	Excellent	Fair	~ 15	4.5
CVD SiC	1	>1315	0.90	Excellent	Fair	0.05 - 0.40	1 - 10
CVD SiC/C	1	>1315	0.88	Excellent	Fair	0.05 - 0.40	1 - 10
HfC-10%TaC	1	>1315	0.70	Excellent	Fair	0.05 - 0.40	1 - 10
MA956	7	>1315	0.57	Poor (oxide)	Fair	27@1100C	15.5
Nb-1%Zr	9	>1315	0.33	Poor (oxide)	Good	41.9	7.54
SiC	10	>1315	0.80	Excellent	Fair	15.1	~ 4.5
SiC/Si	4	>1315	0.88 - 0.93	Excellent	Fair	~ 15	4.2
Silicon Nitride	2	>1315	0.87	Excellent	Fair	29.5	3.4
W-40%Re	11	>1315	0.22	Good (residue)	Excellent	~ 100	~ 5
Woven C/SiC	3	>1315	0.86	Excellent	Fair	0.05 - 0.40	1 - 10
Zirconia	8	>1315	0.17	Poor	Poor	4	10.5
ZrB2/SiC	2	>1315	0.78	Excellent	Fair	0.05 - 0.40	1 - 10

Manufacturers:

- (1) Ceramic Composites, Inc.
- (2) Advanced Ceramics Research
- (3) Refractory Composites, Inc.
- (4) INEX, Inc
- (5) Teledyne, Inc
- (6) Advanced Ceramics
- (7) Inconloy
- (8) Vesuvius McDanel
- (9) Cabot Performance Materials
- (10) Vesuvius Neomelt
- (11) Rhenium Products
- (12) Zircar

10.2 WEIGHTING OF CRITERIA

In order to quantitatively compare the candidate materials, a weighting system that accounted for the importance of each material property was created. In each property category, the candidate materials were ranked, with the best materials receiving a "4.0" for the category, and the worst receiving a "0.0". Each material property was also weighted and assigned a percentage that reflected its importance in the overall design, with the total of the percentages equaling 100%.

The criteria were weighted as shown in Table 25.

Table 25 Material Property Weighting

Material Property	Weighting
Melting Temperature	20%
Thermal Shock Resistance	20%
Emissivity	20%
Oxidation Resistance (with coating if necessary)	20%
Machinability	10%
Thermal Conductivity	5%
Coefficient of Thermal Expansion	5%

Melting temperature, thermal shock resistance, and emissivity were given the highest weighting percentages because they are the most vital properties of the emitter. If the emitter material does not meet the minimum temperature requirements of 1300°C, it will melt during use and destroy the rest of the TPV generator. If the emitter material were to

break due to thermal shock, it would be useless and it would expose the rest of the TPV generator, including the sensitive TPV cells, to the combustion gases. If the material does not meet the minimum emissivity requirements, then the efficiency of the TPV generator is diminished and the design is useless. Oxidation resistance is important since it affects the life of the emitter and dictates how often it needs to be replaced. Typically, oxide coatings enhance emissivity, so minor oxidation is not a tremendous concern and can even be a benefit. Machinability of the material affects the cost of production and can in extreme cases prove so poor that a piece can not be made. Coefficient of thermal expansion influences the design, but it does not prevent a design from being built as long as tolerances are included for the individual materials. Thermal conductivity ordinarily influences efficiency, but in this case the emitter is thin-walled, and at high temperatures will not impede heat transfer unless it is a very poor conductor.

Table 26 displays the candidate materials and their rankings:

Table 26 Weighted Quantitative Material Comparison

Weighting Factor	Melting Temperature 20%	Thermal Shock Resistance 20%	Emmissivity 20%	Oxidation Resistance 20%	Machinability 10%	Thermal Conductivity 5%	Thermal Expansion 5%	Ranking 0.00 - 4.00
Alumina	4	4	0	4	1	3	3	2.80
BN	4	4	0	2	4	3	4	2.75
C-103	4	1	0	1	2	4	1	1.65
C/SiC w/ SiC Overcoat	4	4	4	3	2	2	3	3.45
CVD HfC	4	4	1	1	2	1	2	2.35
CVD SiC	4	4	4	1	2	1	2	2.95
CVD SiC/C	4	4	3	3	2	1	2	3.15
HfC-10%TaC	4	4	1	1	2	1	2	2.35
MA956	4	1	0	1	2	3	1	1.60
Nb-1%Zr	4	1	1	1	3	4	1	1.95
SiC	4	4	3	3	1	2	3	3.15
SiC/Si	4	4	4	3	2	2	3	3.45
Silicon Nitride	4	4	3	3	3	2	3	3.35
W-40%Re	3	1	0	1	4	4	2	1.70
Woven C/SiC	4	4	3	3	2	1	2	3.15
Zirconia	4	0	0	4	1	1	1	1.80
ZrB2/SiC	4	4	2	3	2	1	2	2.95

10.3 EMITTER MATERIAL

Based on the material selection process, two materials were chosen for testing in the TPV generator. The silicon carbide in a silicon matrix composite from INEX, Inc. had the second highest emissivity of the materials evaluated, ranging from 0.89 to 0.93. The emissivity of SiC/Si improves with use because a stable high emissivity oxide coating builds up on its exposed surfaces. Its only apparent weakness is that at extremely high temperatures (1400°C and above) its silicon matrix may begin to melt, but this is not expected to affect the performance of the material in this application since operating temperatures will only reach 1300°C. INEX, Inc. produces one inch diameter pieces of SiC/Si for special orders only. The appropriate sized material was not received by the conclusion of the project.

A second material, a carbon fiber in a silicon carbide matrix with silicon carbide overcoat composite, was ordered from Ceramic Composites, Inc. (CCI). Emissivity testing indicated that this sample achieved an emissivity of 0.95 across a wide range of temperatures (300K-1500K). Since emissivity is a surface phenomenon, the SiC overcoat directly influenced the overall emissivity of the composite emitter. The surface texturing due to the carbon fiber weave invariably contributed to the high emissivity as well. This material has two significant advantages over other composites. CCI understands the requirements of the emitter, and has tailored the properties of the composite to meet the design requirements. Additionally, CCI has developed a new technique for creating composite ceramics that reduces both the amount of lead time necessary to build the composite and the cost of the composite. Reverse thermal gradient

(RTG) Chemical Vapor Infiltration (CVI) has been used as a breakthrough technology for fabricating erosion resistant, ceramic matrix composite (CMC) rocket nozzles. Cost savings are inherent with the RTG CVI process because of a ten-fold reduction in the time to process materials compared to conventional CVI. Additionally, the RTG CVI process has demonstrated that it can produce ceramic composites with much greater densities than previously. This added density improves the chances that the combustion gases passing through the emitter will not escape through the emitter walls and impinge on the delicate TPV cells. Manufacturer testing has demonstrated that CCI composites produced by this method possess the following properties:

- Dense matrix composition to increase linear elastic limit
- Adherent, oxidation resistant surface
- Thermal shock resistance
- Higher chamber pressures
- Higher elastic fracture (proportional limit) strengths
- Increased erosion resistance
- Faster and lower cost processing [21]

10.4 ALTERNATIVE DESIGN

Alternative designs could be used to simplify some of the material problems encountered during material selection. The combustion gases used to heat the emitter are the primary source of concern for emitter corrosion. At high temperatures, few materials can fully withstand the corrosion encouraged by impinging combustion gases. An

alternative would be to coat the interior of the emitter with an oxidation resistant coating such as platinum, a coating that would still encourage heat transfer from the gases to the external surface of the emitter.

Corrosion of the outside of the emitter is another concern. At 1300°C many materials corrode even in a free air environment. More effective emitters could be used if this external environment were a vacuum. Graphite is an example of a material that can exhibit extremely high emissivities (~ 0.95) when textured. Unfortunately, graphite sublimates at high temperatures in a free air environment. Controlling the external environment of the emitter would broaden the field of candidate materials.

11.0 CONCLUSIONS

The goal of this project was to conduct material selection for the emitter in a TPV generator. Material selection was aimed at meeting the specific requirements of a TPV emitter. The following sections summarize the findings.

11.1 MATERIAL RECOMMENDATIONS

The Naval Academy's thermophotovoltaic generator design placed stringent requirements on the emitter material. Specifically, the emitter material must withstand temperatures of 1300°C, possess an emissivity of at least 0.90, have a high oxidation and thermal shock resistance, have a high coefficient of thermal conductivity, and be machinable.

Melting temperature and oxidation resistance were tested simultaneously in a high temperature furnace. Each material sample was exposed to a free air environment at 1315°C. Emissivity testing was conducted at NASA Lewis Research Center in Cleveland, Ohio on a limited number of samples. Thermal shock resistance was evaluated at Technology Assessment & Transfer, where samples were individually shocked using an acetylene torch. Coefficients of thermal conductivity for the samples were obtained from reference materials. Finally, machinability was evaluated by machine shop personnel as they cut samples of each material.

Two samples performed significantly better than the others. The first sample is a carbon fiber in a silicon carbide matrix with silicon carbide overcoat composite (from Ceramic Composites Incorporated) which recorded the highest emissivity of 0.95.

Throughout the tests, this material demonstrated excellent emitter material potential, receiving a final score of 3.45 on a 4.00 scale.

The second sample is a silica bonded silicon carbide (from INEX Incorporated). This sample recorded an emissivity of 0.89 before high temperature exposure, and the second highest emissivity of 0.93 following high temperature exposure. This trend indicates that the emissivity of the material will improve with time and use as an oxide coating develops on its surface.

Both materials have been identified as emitter candidate materials for future testing and design.

11.2 FUTURE CONSIDERATIONS

Additional testing should be conducted on the selected emitter materials. To date, material testing has consisted of individual tests conducted with small samples. Emitters should be constructed out of both materials for full scale material testing. Material properties such as thermal shock resistance can be greatly influenced by the geometry of the test sample, so additional testing is needed to verify that the larger emitter configuration does not alter the results of the emitter material experiments.

Published data that was used to evaluate the two emitter materials should be verified through experimentation. This testing ensures that the data accurately reflect the properties of the specific samples used in this project. Following these tests, if the emitter materials continue to meet the emitter requirements, they should be tested in the

actual TPV generator test cell. Service testing is the only true test of a material's performance under exact conditions.

11.3 PROJECT CONCLUSIONS

Two materials were discovered that met the requirements of the Naval Academy's TPV emitter. C/SiC w/ SiC overcoat from Ceramic Composites Incorporated and SiC/Si from INEX Incorporated exhibited the required melting temperatures, emissivities, oxidation resistances, thermal shock resistances, machinability, thermal expansion, and thermal conductivity expected in an emitter material. Both materials have been ordered in the proper configuration for further material testing and eventual service testing.

WORKS CITED

1. Borowsky, E. W. and R. J. Dziendziel (eds). "Thermophotovoltaics (TPV) Primer."
2. DeWitt, David P. and Frank P. Incropera. Introduction to Heat Transfer. New York: John Wiley & Sons, 1996.
3. Fraas, Lewis M., et al. "SiC IR Emitter Design for Thermophotovoltaic Generators." Second Annual National Renewable Energy Laboratory Conference on Thermophotovoltaic Generation of Electricity, 1995.
4. Lowe, Roland A., et al. "The Effect of Thickness and Temperature on the Performance of Thin Film Selective Emitters for Thermophotovoltaic Applications." IECEC Paper No. RE-14, 1995
5. Loughin, Stephen, et al. "Radioisotope Thermophotovoltaic Generator for Space Power Applications." IECEC Paper No. AP-302, 1995.
6. Stone, K. W. "System Performance of a Solar Thermophotovoltaic System for Space and Terrestrial Applications." IECEC Paper No. AP-20, 1995.
7. Benner, John P. and Timothy J. Coutts. AIP Conference Proceedings 321: The First NREL Conference on Thermophotovoltaic Generation of Electricity. New York: American Institute of Physics, 1995.
8. Erickson, Timothy. "Design and Construction of a Thermophotovoltaic Energy Conversion System Using Combustion Gases from a T-58 Gas Turbine." Trident Scholar Report. U.S. Naval Academy. May 1997.
9. Smith, William F. Principles of Materials Science and Engineering. New York: McGraw-Hill, 1996.
10. Benjamin, David, ed. Metals Handbook Ninth Edition. Metals Park, OH: American Society for Metals, 1980.
11. Somiya, Shigeyuki. Advanced Technical Ceramics. San Diego: Academic Press, Inc., 1984.
12. Chawala, K.K. Ceramic Matrix Composites. New York: Chapman & Hall, 1993.
13. Banks, Bruce A., et al. "Arc-Textured Metal Surfaces for High Thermal Emittance Space Radiators." NASA TM-100894, 1988.

14. Banks, Bruce A. "Ion Beam Applications Research - a 1981 Summary of Lewis Research Center Programs." NASA TM-81721, 1981.
15. INCOLOY alloy MA 956 Product Literature. Inco Alloys International, Inc.
16. Nair, Shanti V. and Karl Jakus, eds. High Temperature Mechanical Behavior of Composites. Boston: Buterworth-Heinemann, 1995.
17. Silica Bonded Silicon Carbide Product Literature. Vesuvius Neomelt.
18. Siliconized Silicon Carbide Product Literature. INEX Incorporated.
19. Rutledge, Sharon K., et al. "The Effectos of Atomic Oxygen on the Thermal Emittance of High Temperature Radiator Surfaces." NASA TM-103224, 1989.
20. Rutledge, Sharon K., et al. "Thermal Emittance Enhancement of Graphite-Copper Composites for High Temperature Space Based Radiators." NASA TM-105178, 1991.
21. Ceramic Composites Incorporated Product Literature.

REFERENCES

- Banks, Bruce A., et al. "Arc-Textured Metal Surfaces for High Thermal Emittance Space Radiators." NASA TM-100894, 1988.
- Banks, Bruce A. "Ion Beam Applications Research - a 1981 Summary of Lewis Research Center Programs." NASA TM-81721, 1981.
- Benjamin, David, ed. Metals Handbook Ninth Edition. Metals Park, OH: American Society for Metals, 1980.
- Benner, John P. and Timothy J. Coutts. AIP Conference Proceedings 321: The First NREL Conference on Thermophotovoltaic Generation of Electricity. New York: American Institute of Physics, 1995.
- Borowsky, E. W. and R. J. Dziendziel (eds). "Thermophotovoltaics (TPV) Primer." 1994.
- Ceramic Composites Incorporated Product Literature, 1997.
- Cheremisinoff, Nicholas P., ed. Handbook of Ceramics and Composites. Vol 1 & 2. New York: Marcel Dekker, Inc., 1990.
- Chawala, K.K. Ceramic Matrix Composites. New York: Chapman & Hall, 1993.
- DeWitt, David P. and Frank P. Incropera. Introduction to Heat Transfer. New York: John Wiley & Sons, 1996.
- DiFilippo, Frank, and Michael J. Mirtich. "Automated Data Acquisition and Processing for a Hohlraum Reflectometer." NASA TM-101393, 1988.
- DiFilippo, Frank, et al. "Total Hemispherical Emittance Measured at High Temperatures by the Calorimetric Method." NASA TM-102322, 1989.
- Erickson, Timothy. "Design and Construction of a Thermophotovoltaic Energy Conversion System Using Combustion Gases from a T-58 Gas Turbine." Trident Scholar Report. U.S. Naval Academy. May 1997.
- Fordham, R. J., ed. High Temperature Corrosion of Technical Ceramics. New York: Elsevier Science Publishers Ltd., 1990.
- Fraas, Lewis M., et al. "Development of a Small Air-Cooled "Midnight Sun" Thermophotovoltaic Electric Generator." Second Annual National Renewable Energy Laboratory Conference on Thermophotovoltaic Generation of Electricity, 1995.
- Fraas, Lewis M., et al. "SiC IR Emitter Design for Thermophotovoltaic Generators." Second Annual National Renewable Energy Laboratory Conference on Thermophotovoltaic Generation of Electricity, 1995.
- Hahn, H. Thomas, ed. Composite Materials: Fatigue and Fracture. Philadelphia: ASTM, 1984.
- INCOLOY alloy MA 956 Product Literature. Inco Alloys International, Inc.
- Lai, George Y. High-Temperature Corrosion of Engineering Alloys. Materials Park, OH: ASM International, 1990.
- Lindler, Keith W., et al. "The Design and Construction of a High Temperature Photon Emitter for a Thermophotovoltaic Generator." U.S. Naval Academy, 1995.
- Loughin, Stephen, et al. "Radioisotope Thermophotovoltaic Generator for Space Power Applications." IECEC Paper No. AP-302, 1995.

- Lowe, Roland A., et al. "The Effect of Thickness and Temperature on the Performance of Thin Film Selective Emitters for Thermophotovoltaic Applications." IECEC Paper No. RE-14, 1995.
- Lynch, J. F., ed. Engineering Property Data on Selected Ceramics. Columbus, OH: Metals and Ceramics Information Center, Battelle, 1979.
- Nair, Shanti V. and Karl Jakus, eds. High Temperature Mechanical Behavior of Composites. Boston: Buterworth-Heinemann, 1995.
- Resnick, Robert and David Halliday. Physics. New York: John Wiley & Sons, Inc., 1966.
- Richerson, David W. Modern Ceramic Engineering. New York: Marcel Dekker, Inc., 1992.
- Rutledge, Sharon K., et al. "The Effectos of Atomic Oxygen on the Thermal Emittance of High Temperature Radiator Surfaces." NASA TM-103224, 1989.
- Rutledge, Sharon K., et al. "High Temperature Radiator Materials for Applications in the Low Earth Orbital Environment." NASA TM-100190, 1987.
- Rutledge, Sharon K., et al. "Thermal Emittance Enhancement of Graphite-Copper Composites for High Temperature Space Based Radiators." NASA TM-105178, 1991.
- Savage, G. Carbon-Carbon Composites. New York: Chapman & Hall, 1993.
- Schroeder, K. L., et al. "A Parametric Study of TPV Systems and the Importance of Thermal Management in System Design and Optimization." IECEC Paper No. AP-195, 1995.
- Silica Bonded Silicon Carbide Product Literature. Vesuvius Neomelt.
- Siliconized Silicon Carbide Product Literature. INEX Incorporated.
- Smith, William F. Principles of Materials Science and Engineering. New York: McGraw-Hill, 1996.
- Somiya, Shigeyuki. Advanced Technical Ceramics. San Diego: Academic Press, Inc., 1984.
- Stone, K. W. "System Performace of a Solar Thermophotovoltaic System for Space and Terrestrial Applications." IECEC Paper No. AP-20, 1995.
- Whitcomb, John D., ed. Composite Materials. Philadelphia: ASTM, 1988.